TÜBİTAK

Turkish Journal of Earth Sciences

http://journals.tubitak.gov.tr/earth/

Research Article

Turkish J Earth Sci
(2020) 29: 381-405

doi:10.3906/yer-1909-4

Rheological behaviour in continental and oceanic subduction: inferences for the seismotectonics of the Aegean Region

Massimiliano MAGGINI[1,2], **Riccardo CAPUTO**[1,2,*]

[1]Department of Physics and Earth Sciences, University of Ferrara, Ferrara, Italy
[2]Interuniversity Centre for Three-Dimensional Seismotectonics, CRUST-UR Ferrara, Ferrara, Italy

Received: 04.09.2019 • **Accepted/Published Online:** 17.12.2019 • **Final Version:** 16.03.2020

Abstract: We reconstructed several rheological transects across the Aegean Region, comparing the behaviour in collisional versus subducting settings. We interpolated closely spaced 1D strength envelopes, realized through a dedicated MATLAB script, for determining the shallow lithospheric distribution of brittle and ductile layers. We mainly used literature data and geodynamic considerations to fix the parameters for the rheological modelling and took particular care in reproducing reliable thermal models. The results of the mechanical-rheological model highlighted the following features and differences between the northern continental collision and the southern oceanic subduction settings: i) a slightly shallower brittle-ductile transition (BDT) in the western sectors of the northern transects (~30–33 km) with respect to the southern ones (~40 km); ii) on the contrary, in the central-eastern sectors of the investigated area, corresponding to an extensional tectonic regime, the northern transects have a relatively deeper BDT (about 20–25 km) compared with the southern ones (about 15 km); iii) the occurrence of a thick, deeper brittle layer below the shallowest BDT, in the central-eastern sectors of the northern transects. We suggest that such regional differences are mainly related and attributable to the surface heat flow distribution (which directly affects the geothermal gradient) and to the tectonic and geodynamic context. The results of the rheological modelling in terms of depth extent of the brittle layer(s) have been compared with the depth distribution of available relocated seismicity, showing good agreement with the rheological layering proposed here. Finally, the depth of the shallowest BDT along the transects has been adopted as a constraint for the seismogenic layer thickness. Such information has been used to improve the seismotectonic characterization of selected crustal seismogenic sources crossing the transects, by estimating their maximum potential magnitudes on the basis of their geometrical features and consistency with the rheological layering.

Key words: Rheology, Aegean Region, seismotectonics, modelling, seismic hazard assessment

1. Introduction

Rheological or strength profiles, sometimes also called yield strength envelopes, represent the critical stress conditions that rocks can support as a function of depth (and implicitly of temperature) along a 1D vertical profile (Goetze and Evans, 1979; Brace and Kohlstedt, 1980). The transition from a brittle behaviour in the upper portion of the profile to a mainly plastic one underneath is usually indicated as brittle-ductile transition (BDT) (Scholz, 1988) or brittle-plastic transition (BPT) (Rutter, 1986). This rheological boundary, even though not strictly corresponding to the seismic-aseismic transition, can give reasonable insight on the thickness of the seismogenic layer (Sibson, 1977, 1982) and hence on the maximum possible width of seismogenic sources, which also strongly constrains the maximum magnitude that could affect a region (e.g., Doglioni et al., 2015; Petricca et al., 2015). Providing a contribution on the above issues and particularly on the reconstruction of the BDT for a large sector of the Hellenides represents the major goal of the present research, which could also foster our understanding of the seismotectonics of the Aegean Region (Figure 1). Thanks to the reconstruction of several transects, across both the continental collision and the subduction zone, we also aim at emphasizing the differences in rheological behaviour in the two geodynamic settings, using the Hellenides and the Hellenic Arc as a case study.

The brittle behaviour is usually modelled as frictional sliding (Sibson, 1977; Ranalli, 1995), while the main deformation mechanism assumed for the plastic behaviour is the power-law dislocation creep. In terms of geological record, brittle deformation is typically associated with fractures (either extensional or shear ones), with the corresponding fault rocks, commonly referred to as cataclasites (after Sibson, 1977, 1982), being formed by mechanical abrasion processes, like comminution and

* Correspondence: rcaputo@unife.it

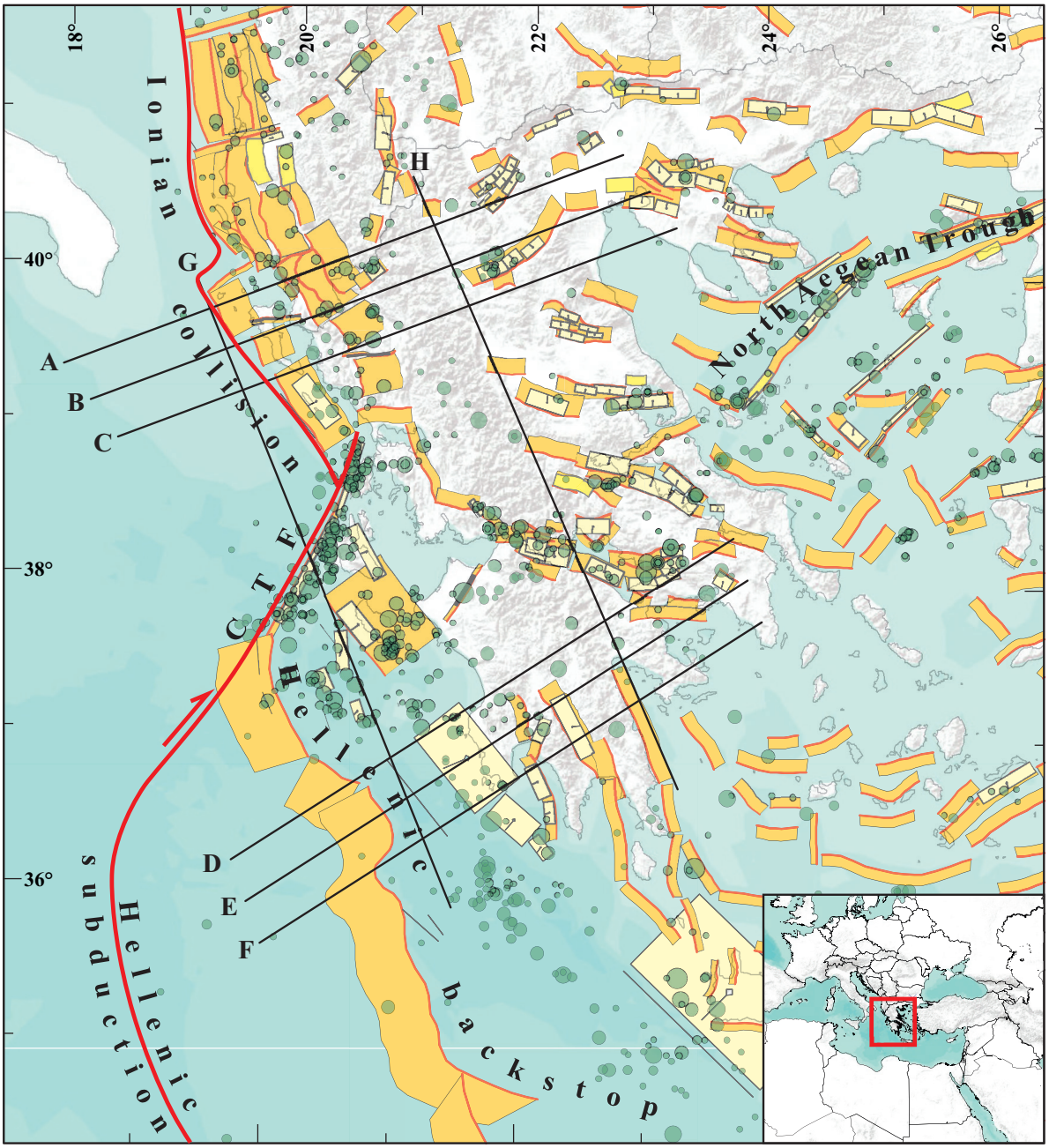

Figure 1. Geodynamic sketch map of the broader Aegean region. Both composite and individual seismogenic sources (CSS and ISS, respectively) from GreDaSS (Caputo et al., 2012) are represented as well as the traces of the transects generated by interpolation of densely spaced 1D rheological profiles. CTF indicates the Cephalonia Transform Fault. Seismicity from NOA catalogue (NOA, 2017). Inset map shows the location of the investigated area.

wearing. On the other hand, ductile deformation along shear zones produces mylonites (Sibson, 1977, 1982) that are in general associated with small-scale folding and pervasive foliation. Around the BDT depth other deformation mechanisms may intervene, such as pressure-solution, recrystallization, and alternating brittle and ductile processes.

Although more complex strength profiles with more than one BDT are possible, for the aims of the present paper devoted to crustal seismotectonic applications, we focus on the shallowest BDT, which usually occurs between 10 and 20 km (Sibson, 1982; Scholz, 1988), though locally deeper (35–40 km). On the other hand, the occurrence of a second deeper brittle layer is unlikely to produce a

significant increase of the seismic hazard, either because at deeper conditions rock strength is far greater than the applied tectonic stresses (in this case, no seismicity at all would occur; e.g., Jackson et al., 2008; Chen et al., 2013) or because the thickness of these deeper brittle layers is commonly reduced (in the order of a few kilometres) and therefore their seismogenic potential is limited. Additionally, in the case of a very deep seismic rupture, say between 50 and 100 km, at events of magnitude comparable to shallow ones, it would be associated with a greater geometric and intrinsic (anelastic) attenuation of the released seismic waves and hence a reduced shaking effect at the surface.

We are also well aware that along the Hellenic Wadati-Benioff zone, at even greater depths (100–200 km), strong events could occur (e.g., Caputo et al., 1970; Makropoulos and Burton, 1984; Papazachos, 1990), but they are far beyond the scope of this paper. However, the role of the subduction zone in generating a thermal anomaly in the upper plate, thus strongly influencing its rheological behaviour, was not ignored in this research and for this reason the numerical modelling has been extended deeper (up to 100 km), though discussion is limited to the shallowest 40–50 km.

We selected the Aegean Region as our study area since it represents an ideal candidate for applying rheological modelling results to seismotectonic issues for several reasons (Figure 1). Firstly, the Aegean realm presents a large spectrum of tectonic regimes (tensile, compressional, transcurrent) and examples of related active structures can be easily found and tested. Secondly, a fair amount of geological (Doutsos et al., 2006; Mountrakis, 2006) and geophysical data is available for the crustal structure (Sodoudi et al., 2006; Makris et al., 2013; Grigoriadis et al., 2016), as well as for the deformation rates (e.g., Hollenstein et al., 2008; Kreemer et al., 2014). Thirdly, the high seismicity rate that characterizes the Aegean Region allows for the recording of robust and independent seismological data (relocated earthquakes depths, focal mechanisms, spatial distribution of seismicity, etc.; Hatzfeld et al., 1995; Resor et al., 2005; Kassaras et al., 2016; National Kapodistrian University of Athens), which, together with additional geophysical constraints (e.g., gravimetry and receiver functions for determining the crustal structure; Tiberi et al., 2001; Tirel et al., 2004; Zelt et al., 2005; Sodoudi et al., 2006; Makris et al., 2013; Kind et al., 2015; Grigoriadis et al., 2016; Sachpazi et al., 2016, among others) can be used for comparison with the rheological modelling results.

2. Tectonic setting

The Aegean Region is one of the most tectonically and seismically active areas in the world, where several microplates, mountain belts, and geological structures play a significant role. The investigated area (Figure 1) is embraced, from the west, by the continental Apulian microplate and the oceanic sector of the Nubian plate; their relative convergence with the Aegean microplate generated the Hellenides-Albanides fold-and-thrust belt and the Hellenic subduction zone; these two contractional domains are separated by the dextral Cephalonia Transform Fault. From the east, the area is characterized by the westwards motion of the Anatolian microplate, which is governed by the dextral North Anatolian Fault Zone merging into the North Aegean Trough. In between, most of continental Greece and the Aegean Sea are affected by a regional lithospheric stretching.

Apulia is commonly considered as a promontory of the African plate and it is currently moving to the NNE at rates of about 4 mm/a with respect to Eurasia according to GPS-derived measurements (e.g., D'Agostino et al., 2008; Nocquet, 2012; Devoti et al., 2014). The Hellenides are the result of the progressive convergence between Gondwana and Eurasia since Mesozoic times. This process has led to the nappe stacking of the interposed microcontinents and oceanic basins characterizing the Neo-Tethyan ocean (e.g., Şengör, 1985; Dercourt et al., 1986; Robertson et al., 1991; Papanikolaou, 2013). As a result, tectonic transport and imbrication has occurred with the diachronic involvement of progressively more external terranes towards the S-SW and the associated development and/or rejuvenation of contractional, NW-SE striking structures (e.g., Jacobshagen, 1986; Mountrakis, 2006; Papanikolaou, 2013). The same orogenic process is deemed to have continued eastwards into the Anatolian region, forming the Pontides and the Taurides belts (e.g., Sengor and Yilmaz, 1981; Robertson and Dixon, 1984; Mountrakis, 1986).

Along the Albanian and northwestern Greek sectors, subduction ended in the late Eocene-early Oligocene (Royden and Papanikolaou, 2011), replaced by a slow (~5 mm/a) continental collision persisting until present. In contrast, south of the Cephalonia Transform Fault, oceanic subduction of the Nubian plate evolved to form the present-day Hellenic Arc associated with a huge low-angle, fast-growing accretionary wedge (Eastern Mediterranean Ridge; e.g., Kopf et al., 2003; Yolsal-Çevikbilen and Taymaz, 2012).

In the back-arc region widespread extension associated with the back-arc effect and the postorogenic collapse (Mercier et al., 1989; Caputo and Pavlides, 1993) began in late Eocene-early Oligocene in the Internal Hellenides (Circum-Rhodope and Axios-Vardar zones) and progressively later in more external (Pelagonian, Pindos, Ionian) zones (Mountrakis, 2006). However, the onset of the current stress field for the broader Aegean Region can be traced back to Middle Pleistocene times (Mercier, 1976;

Le Pichon and Angelier, 1979; Mercier et al., 1989; Caputo and Pavlides, 1993) and it is characterized by an almost N-S minimum stress (σ_3) direction, with a slight rotation of the trajectories towards the NNW-SSE in northwestern Greece. The current N-S crustal stretching, which is greatest in the Corinth Rift (15 mm/a; Briole et al., 2000; Avallone et al., 2004; Caputo et al., 2012), is likely due to an accelerated slab roll-back along the Hellenic Arc (e.g., Faccenna et al., 2014).

At the boundary between the internal extensional realm and the external region mainly undergoing compression, such as close to the Greece-Albania-North Macedonia border and in southern Peloponnesus, a local rotation of the stress trajectories is observed. Indeed, N-S to NNW-SSE striking dip-slip normal faults characterize the areas around Ohrid and Korce to the north and Kalamata and Sparta to the south, documenting an E-W to WSW-ENE extension, as clearly confirmed by seismological (Lyon-Caen et al., 1988; Muço, 1994), geological (Armijo et al., 1992; Reicherter et al., 2011), and geodetic (e.g., Pérouse et al., 2012; Vernant et al., 2014) data and observations (see also Caputo and Pavlides, 2013).

An additional element to take into account for the tectonics of the Aegean Region is the propagation of the dextral, strike-slip North Anatolian Fault Zone into the Aegean Sea (McKenzie, 1972; Taymaz et al., 1991; Jackson, 1994; Taymaz et al., 2004), where it merges into the North Aegean Trough (Taymaz et al., 1991; Koukouvelas and Aydin, 2002), characterized by a transtensional regime. Such a dextral shear motion across the Aegean Region likely started in the Early Pliocene (Armijo et al., 1996).

To summarize, the current kinematic framework and tectonic setting of the broader Aegean Region result from the complex and diachronic interplay of three main geodynamic processes: i) the subduction/collision of the Nubian and Apulian plates; ii) the slab roll-back and sinking of the northward dipping Tethyan oceanic lithosphere and the consequent back-arc extension affecting the upper plate; and iii) the westward motion of the Anatolian block.

3. Thermo-rheological modelling for oceanic and continental lithosphere

For the purpose of thermo-rheological modelling we used the simplified approach first proposed by Brace and Kohlstedt (1980) and then widely applied in the literature (e.g., Ranalli and Murphy, 1987; Ranalli, 1995). Such a method consists of taking into account only the frictional sliding deformation mechanism and the dislocation creep one, corresponding to the brittle and the ductile behaviour, respectively. On the resulting rheological 1D log (Figure 2) the (increasing) depth is on the vertical axis, while the abscissa represents the strength of the rocks expressed as maximum supported differential stress. The shape of the strength envelope is determined (at 100-m vertical steps) by the lesser between the brittle and the ductile strength. The constitutive equation for the frictional sliding mechanism is (Sibson 1977):

$$\Delta\sigma_c = a \,.\, p \,.\, g \,.\, z \,.\, (1 - \lambda_e) \quad (1)$$

where $\Delta\sigma_c$ is the differential stress [Pa], α is the so-called tectonic parameter depending on the orientation of the principal stress axes, ρ is the density [kg m^{-3}] of the overlying rocks averaged over the depth, g is the gravity acceleration [m s^{-2}], z is the depth [m], and λ_e is the Skempton coefficient, which represents the ratio between pore fluid pressure and hydrostatic pressure. Such an equation linearly correlates the strength with the confining pressure (as far as pressure linearly increases with depth) and also makes explicit the dependence of the strength on the fluid pressure. As a general rule, the greater the pore fluid factor is (i.e. the greater the fluid pressure), the lower the shear strength will be, as fluid overpressure causes the well-known effect of diminishing the effective normal stress that can be supported before reaching the critical shear resistance. The tectonic parameter α also plays a major role in the resulting strength, as far as greater values in rock resistance are associated with compressive regimes with respect to tensional ones. Both the pore fluid factor λ_e and the tectonic parameter α also affect the resulting BDT depth as a direct consequence of their influence on the strength (Figure 2). Indeed, a lower strength gradient associated with the brittle behaviour translates into a deeper intersection with the power-law creep curve. This is the case, for instance, for normal-faulting regimes characterized by low strength values but a relatively deeper BDT.

The equation for the ductile behaviour is the one representing the dislocation creep mechanism, commonly referred to as power-law creep (Ranalli, 1995):

$$\Delta\sigma_c = \left(\frac{\dot{\varepsilon}}{A}\right)^{\frac{1}{n}} \cdot e^{\frac{E}{R \cdot n \cdot T(z)}} \quad (2)$$

where $\dot{\varepsilon}$ is the strain rate [s^{-1}], A the power-law parameter [Pa^{-n} s^{-1}], n the power-law exponent, E the activation energy [J mol^{-1}], R the Boltzmann constant, and T is the temperature [K], which is a function of depth (z). As can be observed from Equation (2), dislocation creep has a strong dependence on the geothermal gradient and therefore the calculation of the geotherm is a crucial issue for rheological modelling.

The theoretical models for the temperature gradient are conceptually different for oceanic and continental lithosphere, since independent and different processes and sources of heat transfer characterize the two lithospheric end-members. The geotherm of the oceanic lithosphere is strictly dependent on its cooling age and tends to diminish with time until it reaches a steady-state equilibrium, as

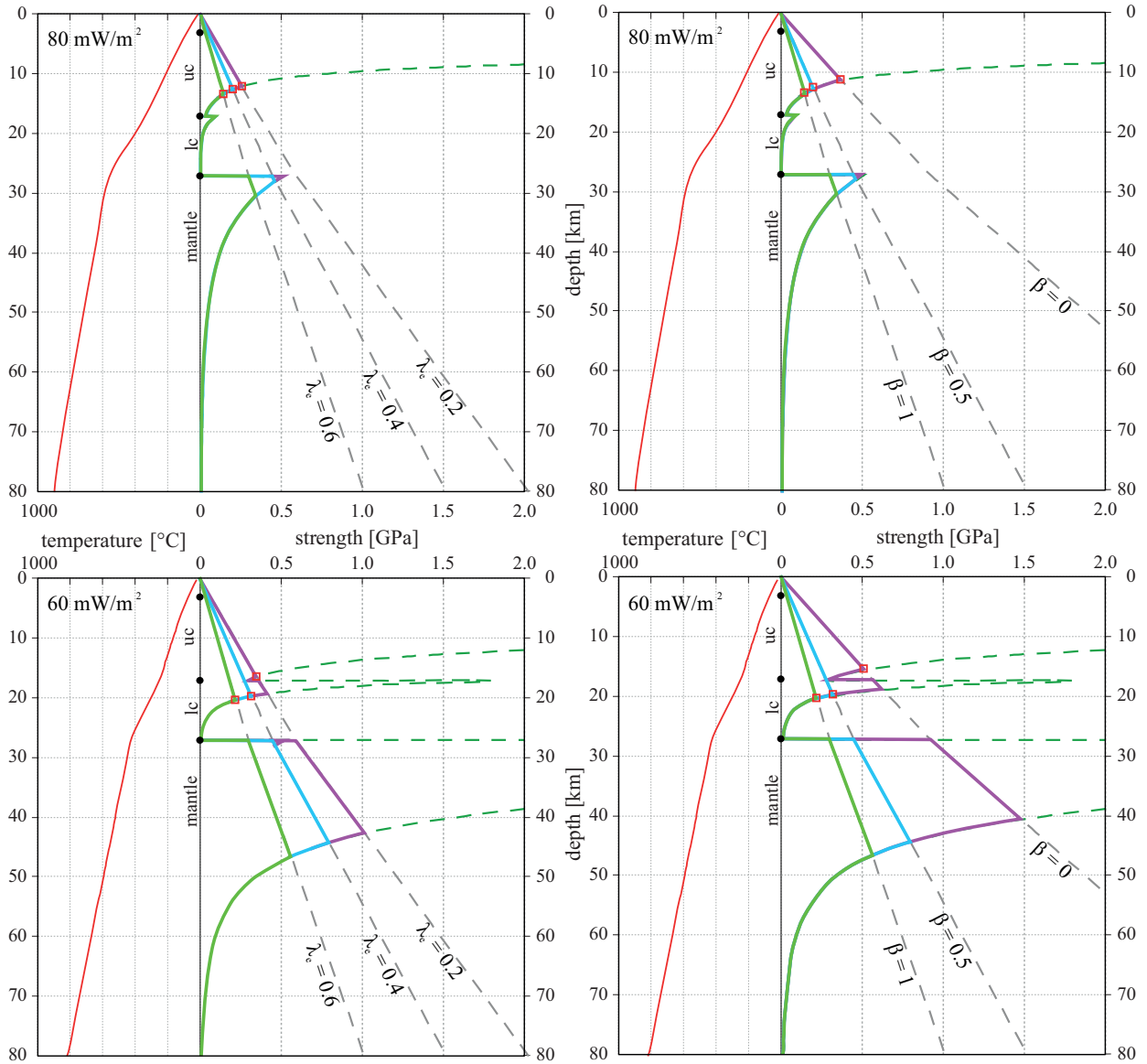

Figure 2. Examples of rheological profiles showing the effects on the strength envelopes of the pore fluid pressure ratio, λ_e (left graphs); and tectonic parameter (stress ratio), β (right graphs), in two different geological settings characterized by high (top graphs) and low (bottom graphs) heat flow values. Dashed lines represent the theoretical brittle and ductile curves. In each diagram the temperature gradient is represented in the left part.

indicated by several models (e.g., McKenzie et al., 2005). On the contrary, the temperature at depth in the continental lithosphere is not just a function of the terrane/platform/plate formation age, but it also strongly depends on the tectonic evolution and, above all, on the occurrence of radioactive elements in the crust, which is clearly related to the lithological composition (see, for instance, Chapman, 1986; Beardsmore and Cull, 2001 among others). Accordingly, the geothermal gradient in the continental lithosphere is the result of the contributions of a greater number of factors and consequently it could show some heterogeneity and variability even at the local scale. The equation for the calculation of the temperature at depth is the steady-state 1D conductive law from Cermak (1982):

$$T(z) = T_0 + \frac{(q_0 - A_0 \cdot D) \cdot z}{k} + \frac{A_0 \cdot D^2 (1 - e^{-z/D})}{k} \quad (3)$$

where $T(z)$ is the temperature [K] at depth z, T_0 is the temperature at the top of the considered layer, q_0 is the surface heat flow density [W/m²], A_0 is the radioactive surface heat production [W/m³], D is an exponential decay constant that is also called characteristic depth

and has the dimensions of a length [m], and k is the thermal conductivity [W/m K]. Such an equation takes into account the radiogenic heat production, which is an exclusive feature of the continental lithosphere, and it is therefore suited to the thermal modelling of such settings. In the case of the oceanic lithosphere the contribution of the radiogenic heat production is negligible and therefore Equation (3) could be simplified as follows:

$$T(z) = T_0 + \frac{q_0}{k} \cdot z \quad (4)$$

The differences in thermal modelling for oceanic and continental lithosphere are also obviously reflected in the resulting strength envelopes. For example, a typical oceanic profile exhibits a single BDT usually occurring in the upper mantle, with the whole thin oceanic crust behaving in a brittle fashion. On the contrary, the continental lithosphere could exhibit profiles with different geometries. In all of them, however, at least the shallowest BDT occurs in the crust, and the upper mantle could behave in a brittle or ductile manner mainly according to the overall thermal gradient.

As mentioned above, this research is devoted to investigating the crustal seismotectonics and therefore the modelling and the discussion of the results will focus on the shallowest BDT and its properties. In order to define this transition, in the event that a deeper second brittle layer occurs, it is assumed that an interposed ductile layer with a thickness of at least 0.5 km is sufficient to mechanically decouple the two brittle layers in terms of seismogenic behaviour and hence seismic potential. In other words, a 0.5-km-thick interposed ductile layer could be considered an adequate 'obstacle' for hindering the propagation of a coseismic rupture from one brittle layer to another one along a hypothetical fault (Rolandone et al., 2004; Beeler et al., 2018), thus making the two hypothetically aligned segments independent of each other in seismological terms.

4. Rheological transects: data and methods

In order to realize the rheological transects, as many as possible literature data from different studies, methods, and sources for defining the values of the input parameters of the constitutive rheological equations have been collected. Whenever possible, data from more than one author or working group and from different scale studies have been considered for each input parameter.

For both overriding and undergoing plates, four lithological/mechanical layers have been assumed, consisting of sedimentary cover, upper crust, lower crust, and upper mantle. The crustal structure, prevailing lithology, and thickness of the above layers have been retrieved mainly from regional-scale studies based on different and integrated geophysical data and methods, such as gravimetry, seismic reflection and refraction profiles, tomographic inversions based on P and S seismic waves arrival times, or receiver functions analyses (Tiberi et al., 2001, Tirel et al., 2004; Zelt et al., 2005; Sodoudi et al., 2006; Makris et al., 2013; Kind et al., 2015; Grigoriadis et al., 2016; Sachpazi et al., 2016, among others). From the analysis of these studies it can be observed that the deepest Moho discontinuity occurs in the axial zone of the Hellenides fold-and-thrust belt with maximum values reaching 40–45 km of depth. On the contrary, the stretched lithosphere of the Northern Aegean and the Hellenic Arc are characterized by a noticeably thinned continental crust, with the Moho being as shallow as 18–20 km in correspondence to the Cycladic core complex.

As concerns the subdivision into upper and lower crust, no regional scale information on the Conrad transition depth is available for the study area. Moreover, the Conrad discontinuity is not as easily detectable by geophysical techniques as the Moho surface, is likely not continuous laterally, and is not unanimously considered by the scientific community as the effective transition between the upper and lower crusts, since its physical meaning is not always clear and it may therefore be related to other variations than lithological ones. Accordingly, the upper-lower crust transition and consequently the thickness of these two layers have been assigned following the global-scale estimates of the lower-to-total crystalline crust thickness ratio proposed by Rudnick and Fountain (1995) and Rudnick and Gao (2003), which is ca 0.4–0.45 (Figure 3).

Finally, for the geometry of the Wadati–Benioff plane used for estimating the thermal anomaly, the recent model proposed by Bocchini et al. (2018) has been adopted. The model is based on seismic and geophysical data and it is in line with the results of the receiver function analysis carried out by Sachpazi et al. (2016).

The lithologies for the different crustal and lithospheric layers have been selected on the basis of the long-lasting tectonic and structural evolution of the Aegean region. We also took into account dedicated palaeogeographic reconstructions from Mountrakis (2006), Ring et al. (2010), and Papanikolaou (2013) and continental-scale works on lithospheric lithologies such as those of Tesauro et al. (2008) and Tesauro (2009). Limestone and metasediments have been selected as the representative lithologies for the sedimentary cover layer (SD in Figure 3); the upper crust of the Aegean plate and Apulian continental block corresponds to a quartzite lithology (UC1 in Figure 3), while for the Nubian plate a more realistic diabase lithology has been assumed (UC2 in Figure 3). The lower crust in the Aegean plate has been associated with a diorite lithology (LC1 and LC2 in Figure 3) and the upper mantle, for both Aegean and Nubian plates, with a peridotite (UM

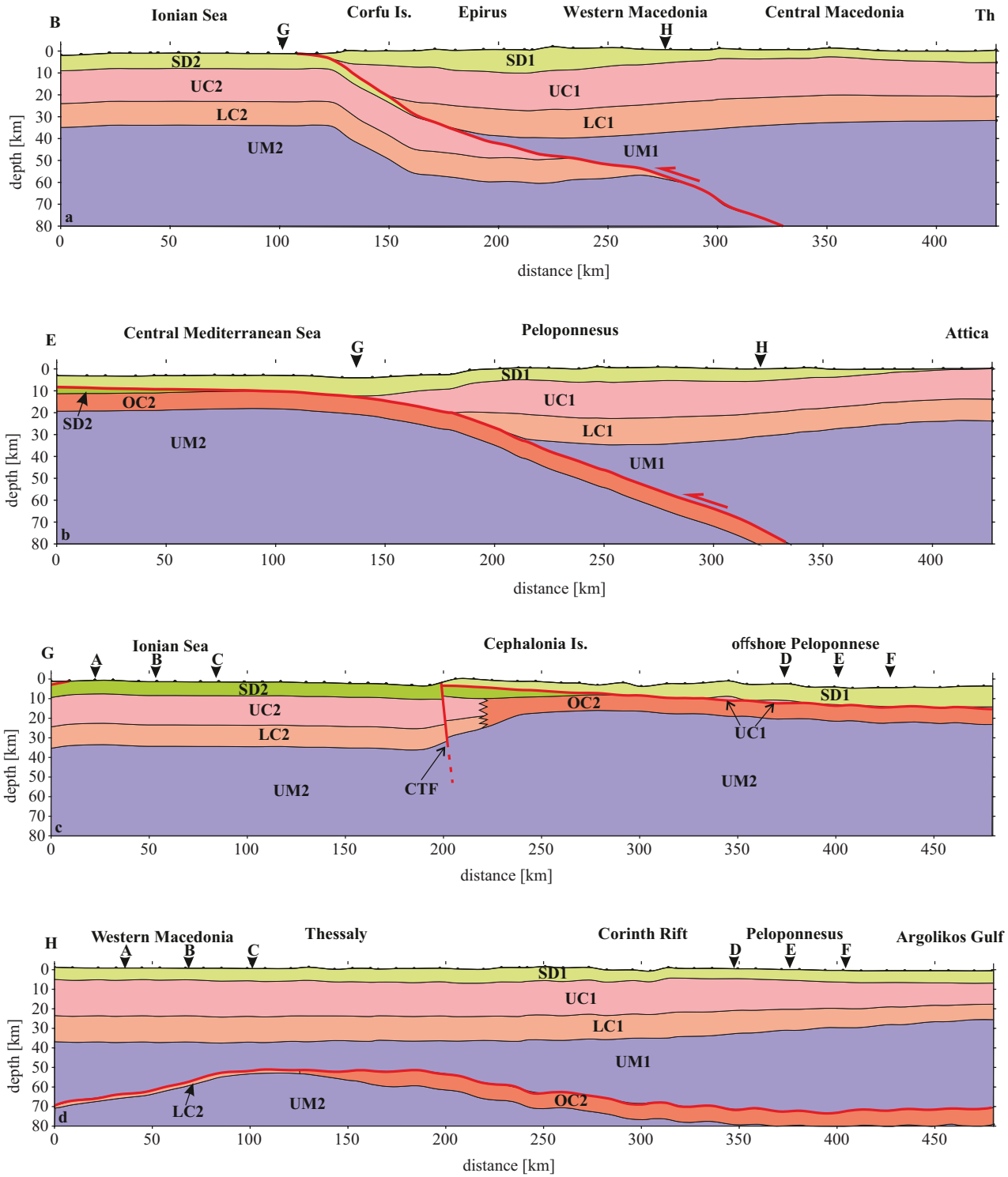

Figure 3. Lithospheric stratigraphy used for the rheological modelling of transects B, E, G, and H (see Figure 1 for locations). Layers labelling: SD = sedimentary rocks; UC = continental upper crust; LC = continental lower crust; OC = oceanic crust; UM = upper mantle; index '1' and '2' refer to the Aegean microplate and Ionian/Nubian plate, respectively. See text for the numerous references considered to draw the lithospheric layering and Table 1 for the corresponding parametric values.

in Figure 3). Some exceptions to these choices occur in the region east of Thessaloniki, around the Mygdonia Graben, where granitoid intrusions are largely mapped, suggesting the use of granodiorite as a more proper representative lithology for the upper crust. All the values for the thermo-rheological parameters (power-law parameter, power-law exponent, activation energy, thermal conductivity, and radiogenic heat production) of the selected lithologies are reported in Table 1, where the selected values come from experimental, analogue, modelling, and review papers provided by many authors.

The strain rate distribution (Figure 4a) has been averaged from a wealth of geodetic-based investigations (Hollenstein et al., 2008; Floyd et al., 2010; Muller et al., 2013; Kreemer et al., 2014). In the broader Aegean region, the highest rates are observed around the Cephalonia Transform Fault, in the Corinth Rift, and along the North Aegean Trough, as well as along the Hellenic Trench south of Crete, with maximum values being up to ~2.0–2.5 × 10^{-14} s^{-1}. Lower values, in the order of 10^{-16} s^{-1}, characterize the central and southern Aegean Sea regions, while continental Greece and Peloponnesus are deforming at intermediate rates of between roughly 1.0 × 10^{-15} and 5 × 10^{-15} s^{-1} (Figure 4a).

Regarding the surface heat flow (Figure 4b), both local and regional scale studies based on point observations and areal interpolation have been considered (Fytikas and Kolios, 1979; Hurter and Haenel, 2002; Cloetingh et al., 2010). Special care has been devoted to averaging and smoothing the different heat flow maps provided by the authors, given the primary influence of this parameter on the resulting thermal regime and related rheological modelling. All the literature sources indicate that the highest heat flow values occur along the Hellenic volcanic arc and in the central Aegean-western Anatolia. On the contrary, low values characterize the outer portion with respect to the Hellenic subduction zone and western continental Greece (Figure 4b).

For the friction coefficient parameter, a reference value of 0.6 has been selected, which is consistent with the classic experiments and review of Byerlee (1968, 1978), and it lies in the interval (0.5–0.8) of the most common values also proposed by Ranalli (1995). In order to account for a lower coupling along major active faults, we assigned slightly lower values down to 0.5 in correspondence to the main seismogenic sources (from the GreDaSS database; Caputo et al., 2012; Caputo and Pavlides, 2013) crossed by our transects. Such a choice is based on the higher wearing, comminution, abrasion, and mineralogically related weakening that occur on seismic shear zones and faults, as documented by, e.g., Collettini and Holdsworth (2004), Chiaraluce et al. (2007), Middleton and Copley (2014).

Regarding the pore fluid factor, a standard 'hydrostatic' value of 0.4 for the Skempton coefficient has been assumed. For peculiar tectonic and geodynamic settings, such as the accretionary prism in the western portion of the study area (Figure 1) and the region around the volcanic arc, we selected slightly higher values up to 0.5. These geological scenarios are likely caused by fluid migrations along preferential pathways such as detachment and flat-ramp thrusts, sediment compaction, limited seepage and consequent overpressures within the accretionary wedge, water release through mineralogical reactions in the mantle wedge beneath the volcanic arc region, etc.

Once numerical values were assigned to all parameters for each of the selected sites along the transects, a systematic methodological workflow was followed. Firstly, based on Equations (1) to (3), the 1D strength envelope was produced by means of a purposely developed MATLAB code (academic license, number 1080014), allowing to calculate along depth the temperature distribution as well as the brittle and ductile strengths. As mentioned above, the thermal perturbation in the upper plate, resulting from the cooling effect of the down-going lithospheric slab, has also been included in the MATLAB code as a function of the distance from the Wadati–Benioff zone.

Table 1. List of parameters used in the rheological modelling for the different lithologies. Values are from Brace and Kohlstedt (1980), Tullis and Yund (1980), Chopra and Paterson (1981), Shelton and Tullis (1981), Çermak and Rybach (1982), Hansen and Carter (1982), Kirby (1985), Doser and Kanamori (1986), Carter and Tsenn (1987), Kirby and Kronenberg (1987), Ranalli and Murphy (1987), Olhoeft and Johnson (1989), Ranalli (1995), Vilà et al. (2010), and Turcotte and Schubert (2014).

Lithology	Layer	A [MPa^{-n} s^{-1}]	n	E [J/mol]	K [W/m K]	A_0 [W/m^3]	ρ [kg/m^3]
Metasediments	SD1, SD2	5.0×10^{-6}	3.0	1.9×10^{5}	3.3	1.84×10^{-6}	2650
Quartzite dry	UC1	6.7×10^{-6}	2.4	1.56×10^{5}	3.0	1.84×10^{-6}	2650
Diorite wet	LC1	3.2×10^{-2}	2.4	2.12×10^{5}	2.91	8.62×10^{-7}	2840
Diabase wet	LC2	2.0×10^{-4}	3.4	2.6×10^{5}	2.64	3.45×10^{-7}	2920
Dunite wet	UM1, UM2	2.0×10^{3}	4.0	4.71×10^{5}	/	/	3350

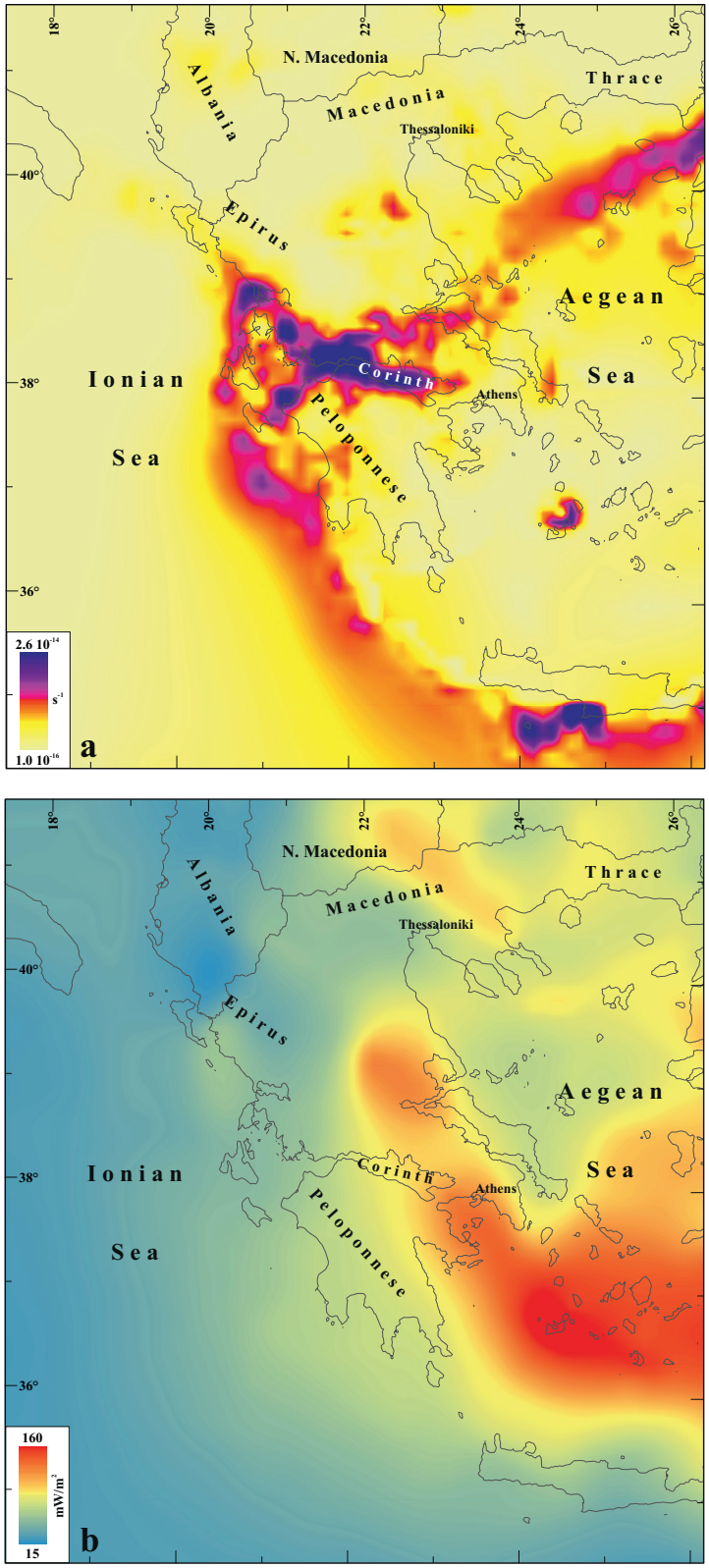

Figure 4. Distribution of strain rate (a) and surface heat flow (b) for the investigated area. The former map is obtained by averaging the results from several geodetic investigations (Hollenstein et al., 2008; Floyd et al., 2010; Muller et al., 2013; Kreemer et al., 2014), while the latter is from local- and regional-scale studies (Fytikas and Kolios, 1979; Hurter and Haenel, 2002; Cloetingh et al., 2010).

The frictional and creep strengths are thus calculated and compared all along the vertical axis and the smaller value among the two is assumed as the maximum shear strength at any given depth. The vertical step for the iteration of the calculations is 100 m, while the total depth covered for each profile is 100 km. The latter choice has been discussed in a previous section while the former represents a reasonable compromise between a useful vertical resolution and computer running time. The intersection between the brittle and the ductile curves determines the BDT depth for each profile. As previously discussed, in the case of the occurrence of a second deeper brittle layer, the interposed ductile layer is considered to be effective in seismically decoupling the two layers only if it attains a minimum thickness of 0.5 km.

The above procedure has been systematically applied to numerous closely spaced sites (mean interdistance of about 10 km) aligned along eight rheological transects across the Aegean region (Figure 1). With the aim of including in our modelling the peculiarities of each site and hence the lateral variations occurring in the Aegean region in terms of lithological vertical stratification, heat-flow, pore fluid pressure, and tectonic setting, we took particular care in the selection of all relevant parameters representative of the specific vertical.

In order to investigate both continental collision and subduction, two sets of three transects have been designed, respectively, from western offshore Corfu Island (western Greece) to Central Macedonia, Greece, and from offshore SW Peloponnesus to Attica (Figure 1). Two additional transects were designed roughly parallel to the Hellenides fold-and-thrust belt in order to cross the two former sets; one runs in an offshore external position and the other from Epirus to Peloponnesus (Figure 1). The crosscutting geometry of the transects has been purposely designed for two reasons: i) intersection points allow to check the consistency between the crossing 2D models and ii) they provide a 3D glimpse of the thermo-rheological characteristics of the investigated region. Transversal and longitudinal transects have a total length of ~430 and 450 km, respectively. The geological sections, represented in Figure 3, clearly show the lateral variability of the lithospheric structure along the selected transects in terms of lithology and thickness of all assumed layers.

In a third working phase, the interspaced 1D logs of ca. 10 km of both strength and temperature were then laterally interpolated for each transect by applying a linear method, which better honours the vertical modelling results for each site. Topography and bathymetry at each interpolated site have been obviously considered. Following this approach, pseudo-2D sections are thus obtained, showing both vertical and lateral variations of the rheological parameters and particularly of the BDT depth and the corresponding strength and temperature.

5. Results of the rheological modelling

The results of the 1D numerical modelling and the subsequent 2D interpolations are shown in Figures 5 to 8. In each figure, the three plots respectively represent the BDT depth (a), the strength at the BDT (b), and the temperature at the BDT (c). For each graph, the black dots indicate the calculated values along the numerous vertical 1D profiles, while the coloured curves indicate their lateral interpolation. Intersections with the other profiles are also shown at the top of the figures. In panel (a) of Figures 5 and 6, the detachment surface separating the two plates is also represented for reference.

As concerns the three northern transects, the BDT in the westernmost 100–120 km ranges at depths between 30 and 33 km (Figure 5a) within the lowermost portion of the Apulian microplate crust (Figure 3a). Due to the overall bending of the lower colliding plate, it progressively deepens eastwards to maximum depths of ca. 53 km. Although such a rheological transition continues further deep in the lower plate, a shallower BDT occurs in the crust of the upper plate in correspondence to Epirus and this rheological setting characterizes the northern transects up to their eastern termination. This shallow BDT occurs at depths varying from 25 to 30 km, to the west, shallowing eastwards up to 20 km in correspondence to Western Macedonia and reaching 15–18 km in the easternmost sector of the transects close to Thessaloniki. It should be noted that in a region between km 300 and 370 of the transects (Figure 5a), the shallow BDTs are at slightly greater depths (ca. 25 km). This local deepening is mainly associated with a decrease of the heat flow and consequently the geothermal gradient in that area (Figure 4a). Indeed, lower temperatures at comparable depths cause an increase of the ductile strength and therefore a deepening of the BDT. Since the area with a relatively low heat flow has an oblique trend with respect to the transects, this feature actually appears at the km 270 in transect A, and only at km 330 in transect C.

As regards the strength at the BDT, a very similar trend to the one observed for the BDT depths is followed (Figure 5c). Indeed, the strengths for the three profiles tend to be steadily between 1000 and 1050 MPa in the western sector within the Apulian platform, progressively increasing as the BDTs deepen eastwards, reaching maximum values of ca. 1800 MPa within the subducted plate. In the Macedonian sector of the transects, where the shallowest BDT occurs in the upper plate, the associated strengths are always between ~200 and ~300 MPa, with the higher values attained in correspondence to the depressed BDTs sector where the heat flow and the geothermal gradient are relatively lower (as discussed above).

As for the temperatures reached at the BDT, they are clearly dependent on the thermal distribution and on the

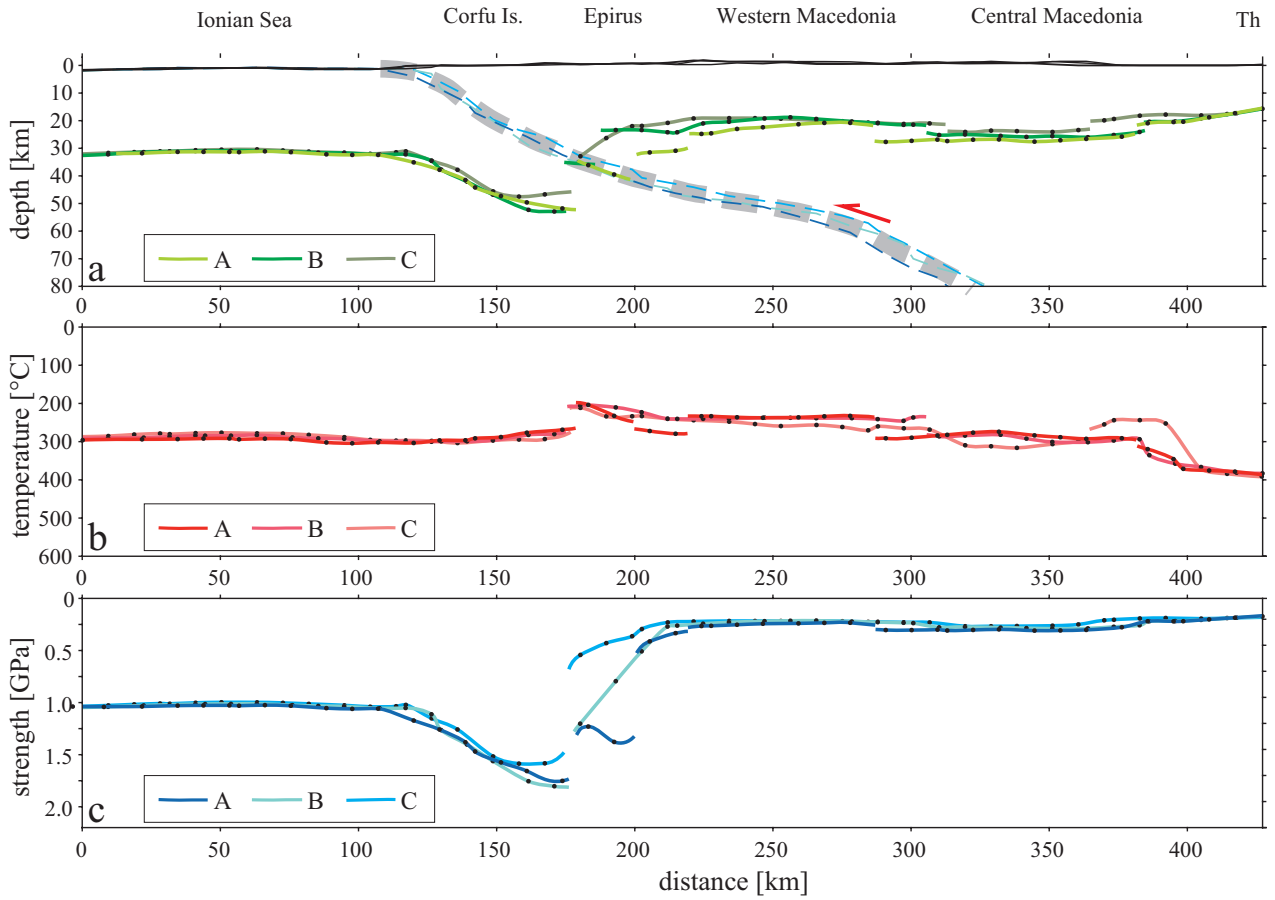

Figure 5. Results of the rheological modelling for the northern set of transects: a) BDT depth; b) temperature at the BDT depth; c) strength at the BDT depth. The overthrust separating the two plates is also represented in (a). Toponyms and geographic references are relative to the central transect B.

depth at which the BDTs occur (Figure 5b). For example, although the BDTs in the Apulian plate are relatively deep (ca. 30 km), the very low geothermal gradients cause the BDT temperatures to remain in the western sector of the transects just below 300 °C. On the other hand, in the central and eastern sectors, the combined effect of a shallower BDT with much higher geothermal gradients leads to comparable BDT temperatures ranging between 210 and 300 °C. The only exception is represented by the easternmost sector in the area around Thessaloniki, where the increase in geothermal gradient overcomes the effect of the BDT shallowing, thus locally increasing the temperatures up to ca. 380 °C.

The southern set of transects (D, E, and F) is also very similar among them in terms of BDT depths (Figure 6a). Indeed, in the westernmost sector of offshore Peloponnesus, the BDT smoothly lies at ca. 40 km, within the mantle of the oceanic crust in the lower plate, and progressively deepens eastwards due to the bending of the African/Ionian oceanic lithosphere undergoing subduction. Similar to the collisional setting, the upper plate is characterized by a shallow BDT laterally fading (WSW-wards) in correspondence to the Peloponnesus peninsula where the transition occurs in the upper crust at depths between 15 and 20 km. A shallowing trend could be observed to the northeast up to minimum values of ca. 10 km in the Saronic Gulf and southwestern Attica, before a final deepening at the easternmost sector of the transects (eastern Attica), with depths of 12–17 km. For this set of transects, too, the role of the heat flow (Figure 4a) and geothermal gradient on the BDT depth is of primary relevance and very evident. Indeed, apart from the lithological differences with respect to the northern collisional setting, a deep BDT in the oceanic crust is also related to the very low temperatures characterizing the cold and old oceanic lithosphere at depth, while the progressive shallowing observed in the upper Aegean microplate is correlated to, and caused by, an increase in the heat flow as the Hellenic volcanic arc is crossed by transects D-E-F where the Aegean crust is thinned due to extension in the back-arc region.

As concerns the strength at the BDT along the southern transects (Figure 6c), the relative values fall between ca. 1.4 and 1.5 GPa in the western offshore sector, where the BDT lies in the oceanic lithosphere, and tend to increase up to maximum values of almost 2.2 GPa as the BDT deepens along the subduction zone. In contrast, where the BDT occurs in the crust of the upper plate the corresponding strength is one order of magnitude lower (100–200 MPa), with minimum values observed in the sector characterized by the shallowest BDT depths (western Attica and Saronic Gulf).

As for the temperature distribution at the BDT (Figure 6b), the highest values are reached in the western sector within the oceanic lithosphere, where they range between 520 and 530 °C, while within the crust of the Aegean microplate, the BDT temperatures are systematically lower, ranging between 260 and 300 °C, with a local peak of ca. 310 °C attained in the easternmost points. Such low temperatures at the BDT of the upper plate are mainly caused by the generally shallow BDT and its lateral variations.

Along orthogonal profiles G and H, the BDT depth clearly follows markedly distinct trends (Figures 7a and 8a). Transect G, lying entirely in a compressional tectonic setting, is characterized by BDT depths of 30–35 km in the northern sector offshore Corfu and Paxos islands, where the transition occurs in the deepest crustal layers of the upper continental plate. To the south the transect crosses the Cephalonia Transform Fault (at km 200), which is associated with an important out-of-plane (i.e. SW-wards) jump of the plate boundary with two further consequences: a sharp deepening (along the transect) of the Wadati–Benioff plane and an abrupt lithological change as far as the lower plate is represented by the Ionian/Nubian oceanic lithosphere (Figure 3c). Accordingly, at the Cephalonia Transform Fault the BDT lies at depths greater than 50 km, rapidly shallowing southwards to depths of about 38 km before slightly deepening again to ca. 45 km. Along the H profile (Figure 8a), which entirely crosses the extensional realm of the internal Aegean region, the BDT always occurs in the upper plate at depths between 11 and 28 km,

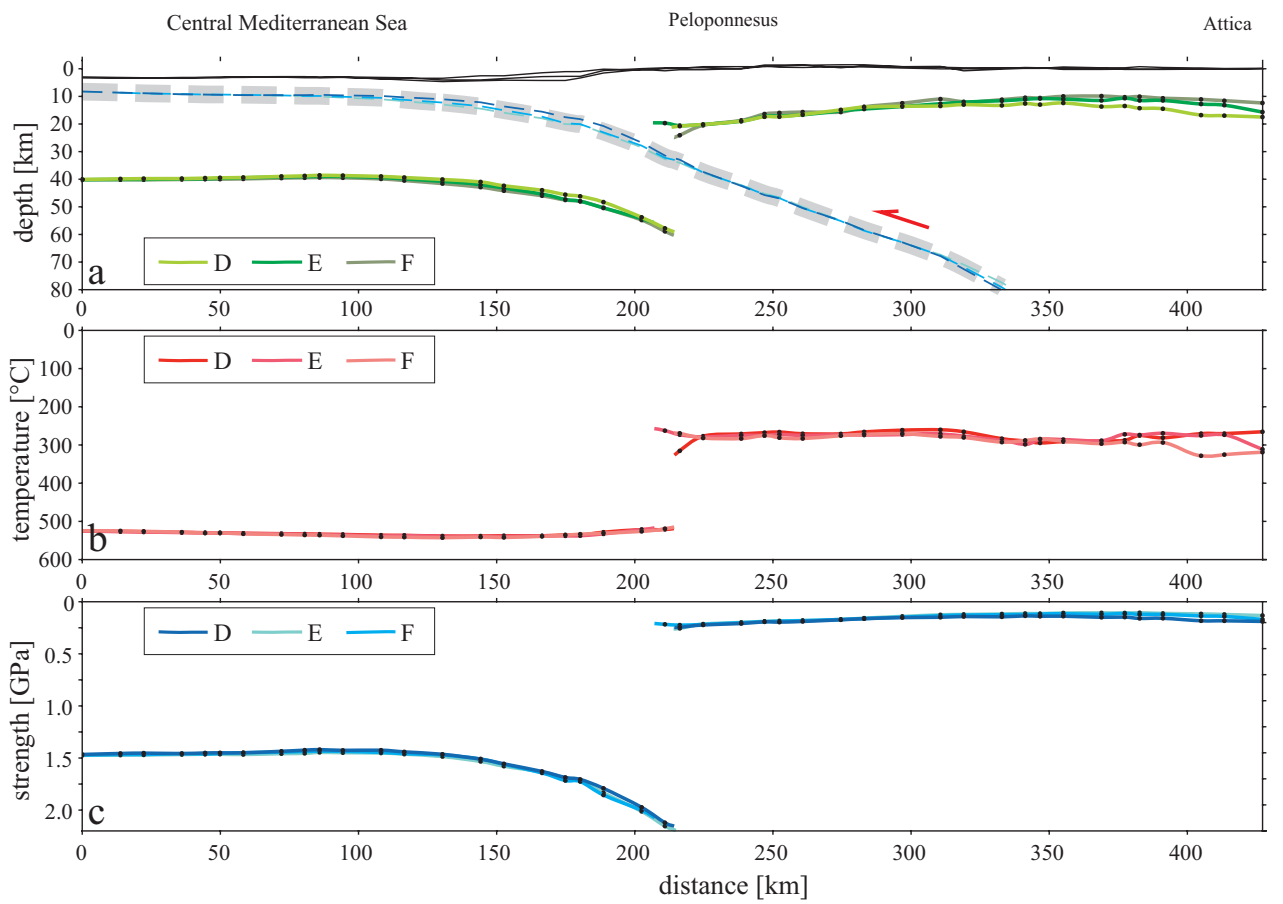

Figure 6. Results of the rheological modelling for the southern set of transects: a) BDT depth; b) temperature at the BDT depth; c) strength at the BDT depth. The overthrust separating the two plates is also represented in (a). Toponyms and geographic references are relative to the central transect E.

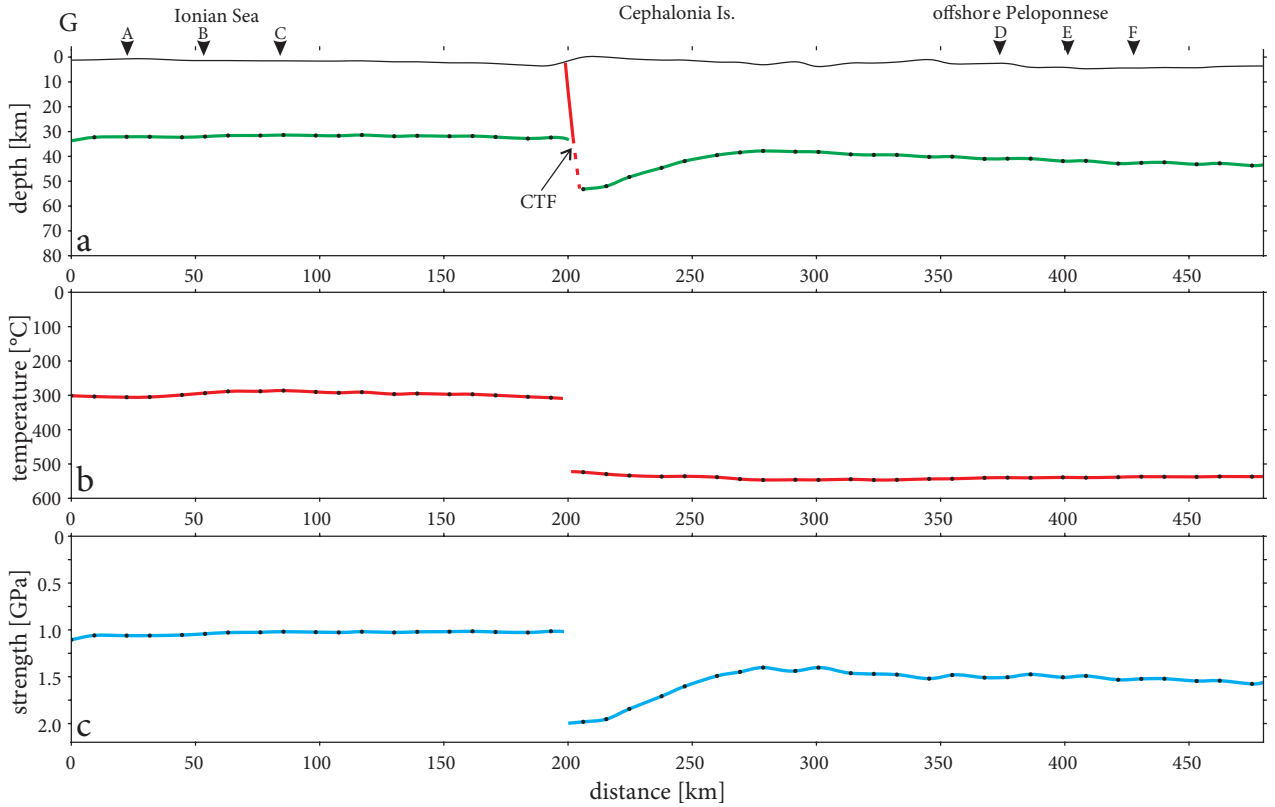

Figure 7. Results of the rheological modelling for transect G: a) BDT depth; b) temperature at the BDT depth; c) strength at the BDT depth.

following a shallowing trend from the northwest (ca. 28 km), at the border between Albania, North Macedonia, and Epirus, to the south-eastern termination (ca. 12 km) in the Argolikos Gulf. In the central sector south of the Corinth Gulf a local deepening to values of ca. 18 km is observed; the BDT depth variations for the H transect are mainly related to heat flow changes (Figure 4a), as it decreases from the northern end to the southern one, with some local (positive) oscillations, as it occurs close to the Corinth rift.

As regards the associated BDT strength (Figures 7b and 8b), for the G profile, they are about 1 GPa in the continental crust north of the Cephalonia Transform Fault, while values of almost 2 GPa are locally attained in conjunction with the deepest BDT located within the subducting oceanic lithosphere. In contrast, along the H profile the values of strength are always much lower due to the shallower BDT and especially to the different tectonic regime. Indeed, it is well known since the findings of Sibson in the 1970s (e.g., Sibson, 1974) that the shear strength in compressional regimes is much higher than in extensional ones. Also, the generally larger heat flows of the eastern transect obviously contribute to this effect. Accordingly, the strength at the BDT in H ranges between ca. 300 MPa (at the northern end) and ca. 120 MPa (at the southern one), with only slight lateral variations.

The trend of the BDT temperatures for transect G (Figure 7b) is characterized by values around 300 °C in the continental crust of the Apulian block (northern sector), sharply jumping to steady values of ca. 520–530 °C in the oceanic lithosphere south of the Cephalonia Transform Fault. The latter trend, which at least in the central-southern sector (km 210–260) seems to be uncorrelated with that of the BDT depths (Figure 7a), suggests once again the great influence that the geothermal gradient (Figure 4a) has on the resulting rheological behaviour and particularly on the ductile one. Indeed, given a fixed lithological and tectonic setting, which could be considered relatively homogeneous south of the Cephalonia Transform Fault, the main factor controlling the depth of the transition is temperature. Indeed, comparing Figures 7a and 7b, the temperature at the BDT is always around 520–530 °C, but the BDT depth is much greater close to the Cephalonia Transform Fault because those temperatures are only reached at greater depths due to the subduction process itself. Finally, along transect H, the BDT temperature shows only small variations between ca. 230 and 300 °C (Figure 8b), and also in this case no clear correlation with

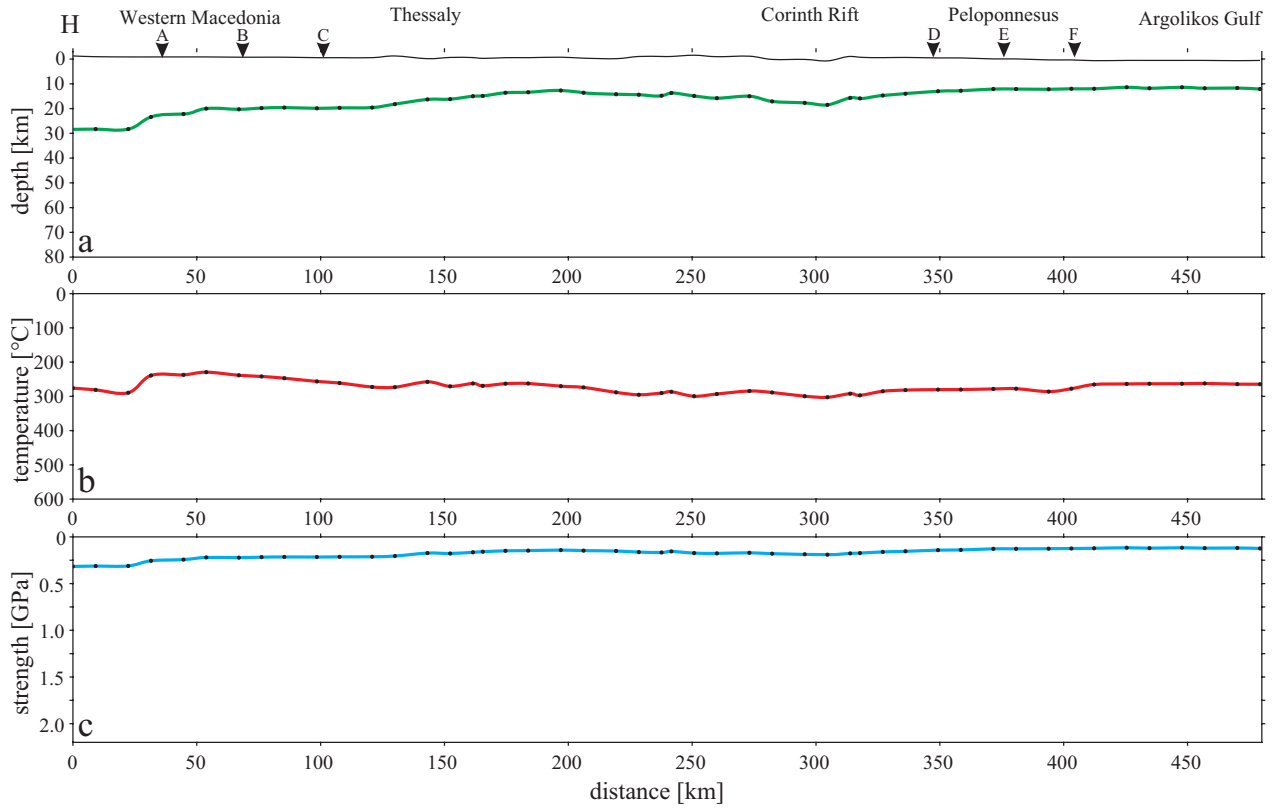

Figure 8. Results of the rheological modelling for transect H: a) BDT depth; b) temperature at the BDT depth; c) strength at the BDT depth.

the BDT depth could be observed at first glance, because of the interplay between lower/higher geothermal gradient (Figure 4a) and deeper/shallower BDT depths (Figure 8a). Those two factors, indeed, tend to compensate each other and, as a result, the BDT temperature remains almost constant, despite the BDT depth lateral changes.

6. Discussion and comparison with seismicity

In the following, the results presented in the previous section are discussed. In particular, the obtained BDT depth is compared with the vertical distribution of well recorded and possibly relocated seismicity. For the sake of simplicity, we are going to focus on profiles B (continental collision), E (oceanic subduction), and G and H (orthogonal transects, respectively belonging to the compressional and extensional tectonic settings). Along these profiles, the correlation with the seismicity distribution at depth is generally in good agreement with the rheological layering and in particular with the depth of the BDT as obtained in this research (Figure 9). As regards the seismicity data used in the comparison, we considered two different catalogues: the first one, from Kassaras et al. (2016), consists of relocated seismicity, and the second one mainly consists of events with $M_w > 3$, for which moment tensors have been calculated by the National Kapodistrian University of Athens. In the catalogue of Kassaras and co-workers, covering a time span of 24 years (1989–2012), the seismicity is relocated through the application of relative relocation techniques such as HypoDD, which allows to substantially reduce the error of the hypocentral depth. In the NKUA catalogue of focal mechanisms (covered period 1995–2019) the good hypocentral depth resolution is guaranteed by the inversion procedures followed to determine the moment tensor solution for each event.

In the northern transect (B; Figure 5) and particularly in the western offshore sector, the BDT is never deeper than 33 km, though it tends to rapidly deepen upon entering the collisional zone in correspondence to the coastal region east of Corfu Island. This behaviour is related to the continental nature of the crust of the undergoing plate and the associated intermediate/felsic typical lithologies (we selected quartzite and granulite for the upper and lower crust, respectively), which tend to yield at lower shear stresses (and therefore at minor confining pressure and depth) with respect to mafic lithotypes. In this brittle volume, however, no seismicity is recorded in either of the two used catalogues (Figure 9a). Such an absence of seismicity might be attributed to the lack of internal

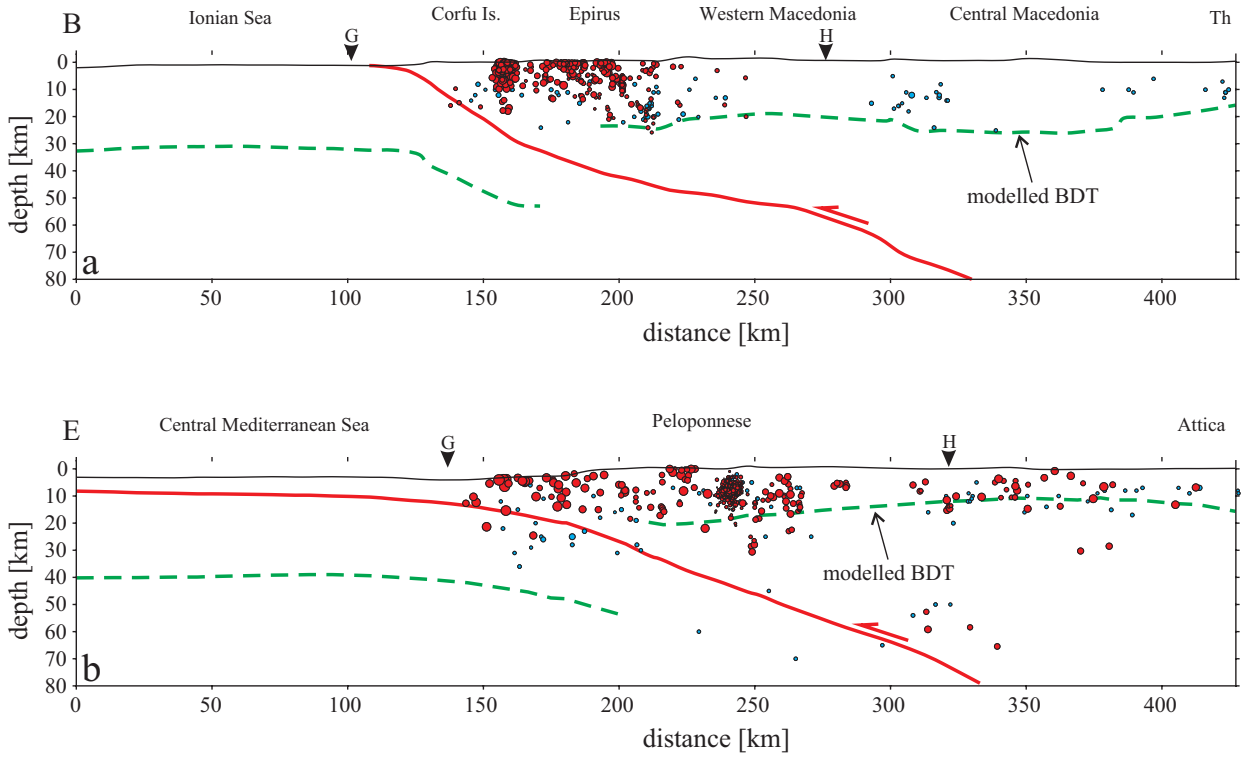

Figure 9. Comparison between the shallowest BDT (green dashed line) with the hypocentral distribution of well-located seismicity along transects B (a) and E (b), respectively. Red and blue circles are from Kassaras et al. (2016) and the National Kapodistrian University of Athens, respectively.

deformation within the Apulian stable platform. Also, closer to the collisional front, the seismicity catalogues might be simply too short in terms of time coverage for recording long return period events, especially in regions characterized by low strain rates (e.g., Kreemer et al., 2014; Chousianitis et al., 2015).

As previously described, in mainland Greece and eastwards, the BDT ranges between 15 and 25 km and it is entirely within the crust of the Aegean microplate (Figure 9a), slightly deeper than what is observed for the corresponding central-eastern sectors of the southern profiles (Figure 9b). This difference is basically due to the lower heat flow characterizing Epirus and western Albania with respect to, for example, Attica and northeastern Peloponnesus (Figure 4a). The comparison between the BDT depth and the distribution at depth of the relocated seismicity (Figure 9a) shows very good agreement (Hatzfeld et al., 1995; Kassaras et al., 2016). The shallower BDT in the eastern sectors is also nicely consistent with the depth distribution of the Kozani-Grevena seismic sequence (mainshock and aftershocks) that occurred in 1995 (e.g., Resor et al., 2005).

Regarding the southern transect (E; Figure 6), the relatively deep transition in the western 180–200 km is due to the oceanic nature of the crust and particularly to its old age (possibly Triassic; van Hinsbergen et al., 2005; Ring et al., 2010 and references therein). It is therefore cold and characterized by a low geothermal gradient; together with the resistant mafic lithologies, this can account for such a deep transition (almost 40 km) that conversely is not necessarily mirrored by a similarly deep seismicity, since the oceanic plate also retains a very high strength (Figure 6c). Accordingly, the almost absent seismicity in the considered catalogues (Figure 9b) might be also explained by the lack of, or very poor, tectonic loading (i.e. not able to overcome the critical differential stress). Whatever the case, seismicity data from the NKUA catalogue show some events as deep as 35 km offshore southwestern Peloponnesus (Figure 9b), which are compatible with the results on the BDT depth given in this work.

The shallow BDT (15–20 km deep) east of Oichalia and Kalamata, Peloponnesus, which is related to the upward jump of the rheological transition from the down-going Ionian-African plate to the overriding Aegean plate, is also in good agreement with the seismicity distribution relocated by Kassaras et al. (2016: Figure 9b). In the back-arc region corresponding to the central-eastern sector of the southern transects some deeper events are recorded at ca. 30 km in depth. These few and minor events ($M \leq 4$), occurring where ductile deformation is expected by our

modelling, are likely due to a local increase in pore fluid pressure leading to a remarkable decrease in brittle strength (Equation (1)), allowing brittle and potentially seismogenic behaviour to occur. This hypothesis is also supported by the fact that the difference between brittle and ductile behaviour (with the latter being theoretically greater than the former) at those depths, along the transect, is actually quite small (Figure 10b) in the back-arc region. Therefore, even a relatively limited decrease in brittle strength would be sufficient to exceed frictional resistance instead of keep deforming in a plastic and aseismic behaviour. The increase of pore fluid pressure in back-arc regions is effectively a common event, because of the continuous release of fluids produced by the slab dehydration, within the context of the subduction process. It should be noted, however, that such variations in fluid pressure likely occur on a small scale, making them not easily detectable and hence not reproducible in our modelling due to the coarser scale of observation. Additionally, such variations may be related to temporal fluctuations of the pore fluid pressure, and since we do not consider the time variable in our model, we are not able to include them in the modelling.

We would like to emphasize that some recorded seismicity deeper than the shallow BDT considered in this paper (Figure 9b) may be associated with a second deeper brittle (and hence potentially seismogenic) layer, for example in the intermediate-lower crust or in the uppermost mantle.

The occurrence of a second deeper brittle layer, below an interposed ductile one, is a feature that has also been inferred from magnetotelluric soundings and the reconstruction of electrical resistivity sections in the area around the Gulf of Corinth (Pham et al., 2000; Chouliaras et al., 1997). Of particular interest are the electrical resistivity sections proposed by Pham et al. (2000) for the eastern Gulf of Corinth on its northern side, which is characterized by a relatively comparable tectonic setting and structural evolution with respect to our study area. The electrical resistivity sections emphasize the presence of an interposed low-resistivity layer at depths between ca. 20 and 30 km, which is interpreted by the authors as a potential ductilely deforming layer. Accordingly, the occurrence of a high-resistivity (brittle) layer deeper than 30 km is in very good agreement with the modelled rheological stratification represented in Figure 10a.

Either in the collisional and subduction settings (Figures 10a and 10b, respectively), deeper brittle layers/volumes could be indeed recognized in the central-eastern sectors of the transects at variable depths from 30 to >80 km. Accordingly, these rock volumes may be potentially seismogenic as well, thus representing the source for the 'deeper' seismicity observed by Kassaras et al. (2016; Figure 9) and also by means of the receiver functions analysis of Sachpazi et al. (2016). Relative to this issue, the comparison between northern and southern transects allows to emphasize some major differences and peculiarities. Firstly, the upper plate in the northern transect (Figure 10a) is systematically characterized by a thicker 'shallow' brittle layer with respect to the southern transect (Figure 10b).

Secondly, in the northern transect, a second continuous, 10- to 18-km-thick brittle layer is observed at depths of 30–40 km within the upper mantle of the Aegean microplate underlying the shallow BDT. With the exception of a small volume underlying Attica there is no such evidence in the southern profile.

Thirdly, in both settings just above the Wadati–Benioff plane, rock volumes characterized by brittle behaviour result from the rheological modelling. They are likely due to the combined effect of the strong thermal cooling induced by the subducting slab, the confining pressure, and lithology. Differences in the latter parameter between the two profiles (Figure 3) explain the different location of these volumes.

Fourthly, in the western sector within the undergoing plate, a second 20- to 25-km-thick continuous brittle layer exists within the collisional setting (northern transect), separated from the shallow one by a ductile layer a few kilometres thick, while only a unique thick brittle layer occurs in the southern profile (Figure 10).

It is worth mentioning that we did not model the lithological variations (for example, due to the intense rock fracturing and mixing up) or the local pore fluid pressure increase and hence the mechanical weakening likely occurring within the shear zone associated with the basal detachment delimiting the accretionary wedge (red line in Figure 10). This could potentially represent an additional rheological transition characterizing the western sector of the investigated area.

Also, as concerns longitudinal profiles G and H, a generally good consistency between the modelling results and the seismicity data could be observed (Figure 11). In particular, profile G seems to perfectly fit all along the projected seismicity from the NKUA moment tensors catalogue and the relocated seismicity of Kassaras et al. (2016). Transect H (Figure 11b) is in a geodynamically more internal position, closer to the volcanic arc and with higher heat flow; it is thus characterized by a thinner brittle layer, which is nicely mimicked by the seismicity distributions of Hatzfeld et al. (1995), Ganas et al. (2012), Kassaras et al. (2016), Mesimeri and Karakostas (2018), and the NKUA moment tensors catalogue. Only a few events occur much deeper than the shallow BDT, between the Corinth Rift and the Argolikos Gulf, and they are possibly related to local increases in pore fluid pressure or very small-scale rheological heterogeneities as previously discussed (Figure 10).

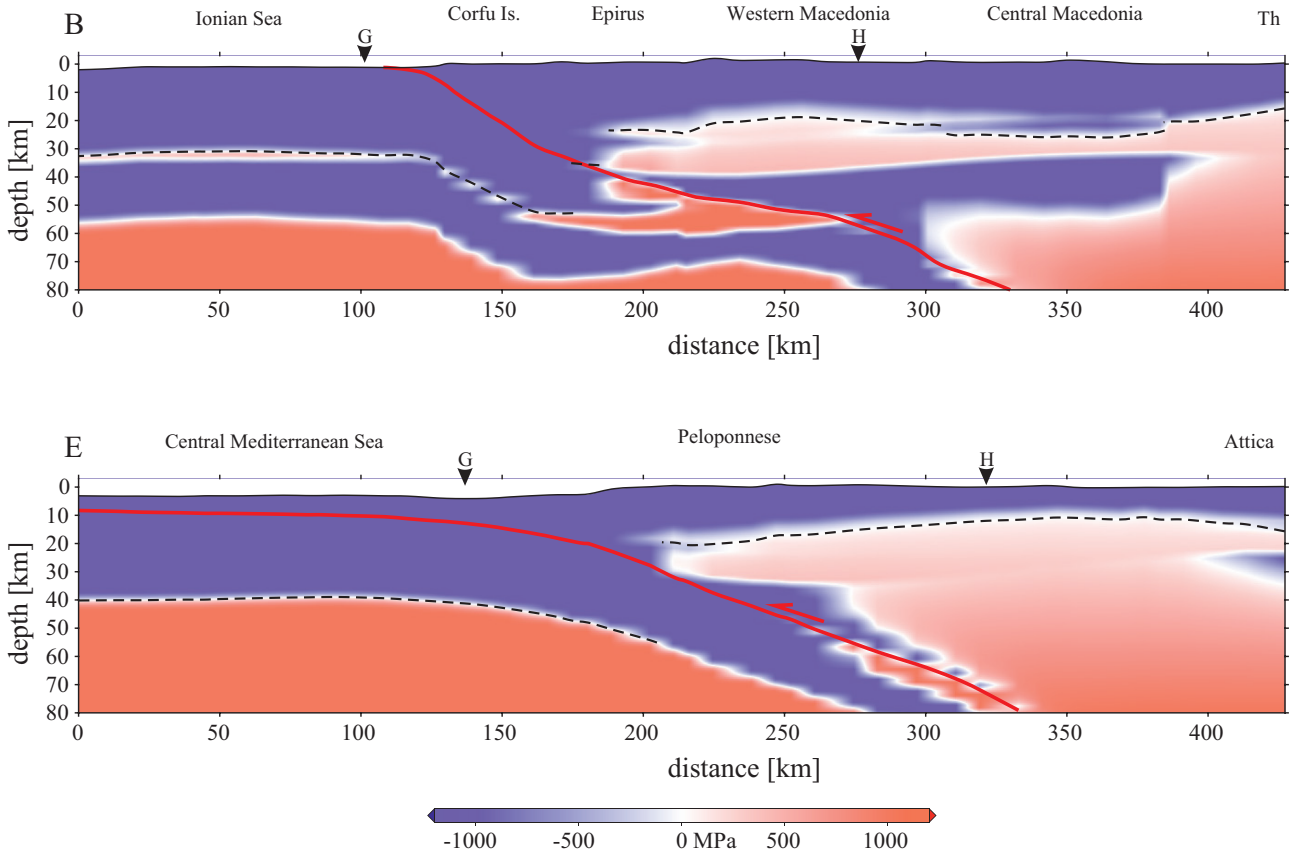

Figure 10. Distribution of brittle and ductile volumes and layers along transects B (a) and E (b), as indicated by the differential strength (brittle minus ductile strength). Blue and red correspond to dominantly brittle and ductile behaviour, respectively, while the whitish colour corresponds to differential strength values close to 0, therefore emphasizing the occurrence of a brittle-ductile transition. The shallowest BDT is marked as a dashed black line.

7. Seismotectonic inferences

In this section we exploit the results obtained from the rheological modelling for seismotectonics purposes and for possibly contributing to the improvement of the seismic hazard assessment of the broader Aegean Region. In particular, the obtained depth of the BDT is used as a constraint to determine, independently of other sources of data, the geometrical (width and secondarily length) characteristics of the seismogenic sources (Caputo et al., 2012) crossed by the transects. In other words, the rheological modelling and the reconstructed 'shallow' BDT depth allow to define the seismogenic layer thickness and therefore also to constrain the maximum credible magnitude. The selected sources are the Offshore Central Corfu Thrust (GRCS610 in GreDaSS; Caputo and Pavlides, 2013) and the Palaeochori Fault (GRIS050) across transect B, and the Kalamata Fault (GRCS562) and the Fili Fault (GRIS450) across transect E. The last three seismogenic sources are close to highly inhabited areas (Kozani, Kalamata, and Athens) and have been also recently reactivated (respectively, the Kozani-Grevena earthquake, 1995; Kalamata earthquake, 1986; and Athens earthquake, 1999). The Offshore Central Corfu Thrust is instead characterized by a lower rate of seismicity and no recorded events are known to have occurred in historical times.

In order to carry out the seismotectonic analysis, several steps have been followed for each selected seismogenic source: i) the BDT depth has been extracted from the rheological model; ii) based on the dip angle (taken from literature data and GreDaSS; Caputo and Pavlides, 2013), the fault width has been calculated; iii) using a length/width ratio equal to 2, the length has also been calculated; iv) applying the empirical relationships of Wells and Coppersmith (1994), the maximum expected magnitude has then been estimated; v) when available, the obtained results have been compared with seismological data (recent seismic sequences, magnitude of the mainshock, depth distribution of the aftershocks). As concerns the use of the empirical relationships, either the width versus magnitude, the surface area versus magnitude, or the length versus magnitude have been applied and then averaged.

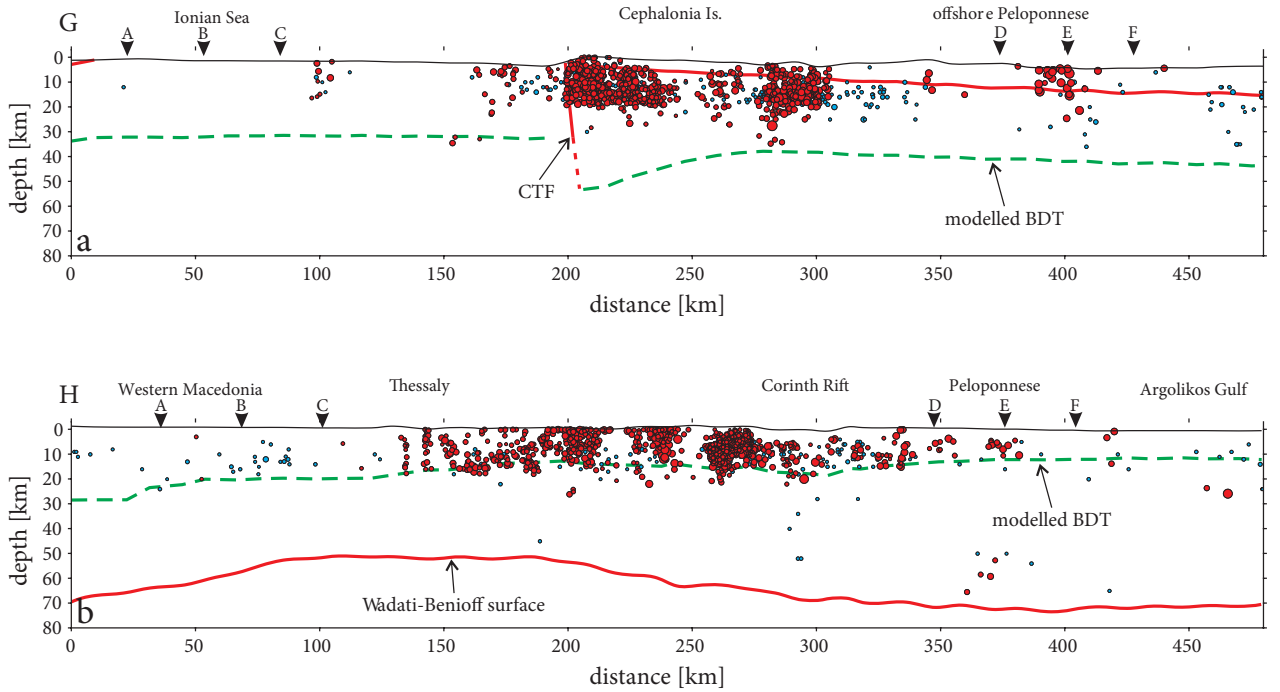

Figure 11. Comparison of the shallowest BDT (green dashed line) with the hypocentral distribution of well-located seismicity along transects G (a) and H (b), respectively. Red and blue circles are from Kassaras et al. (2016) and the National Kapodistrian University of Athens, respectively.

All the results are shown in Table 2 and the relationships between BDT, geometry of the faults, seismicity, and maximum magnitudes are displayed in Figure 12. The compressional tectonic setting affected by the Offshore Central Corfu Thrust (western sector of transect B) is characterized by a low-moderate rate of seismicity with respect to neighbouring regions as, for example, the Cephalonia Transform Fault area and the Corinth Gulf (e.g., Papazachos, 1999; Makropoulos et al., 2012). In this geological and geodynamic context, however, some additional factors should be considered when determining the seismogenic layer thickness for the purposes of seismotectonic modelling and seismic hazard assessment. In fact, even though the BDT in this region occurs at depths of about 40 km (or even deeper; Figure 12), the principal seismogenic sources affecting this region are likely within the accretionary wedge; that is to say, they are delimited down-dip by the mechanical interface (i.e. detachment surface) separating the two plates. It is indeed reasonable to envisage that the main active tectonic structures are connected at depth to the major decollement surface, which may localize deformation and shear, possibly also in an aseismic fashion. Accordingly, the main seismogenic sources are unlikely to crosscut the plate interface and the seismogenic layer thickness is in practice determined by the main detachment itself, provided that the rheological BDT is at least as deep as the plate interface. Given these premises, the seismogenic layer thickness for the Central Offshore Corfu Thrust seismogenic source actually corresponds to the depth of the plate interface, which in the region offshore Corfu is at about 20 km (Figure 12a). Considering such a thickness and an average dip angle of 40° to 45°, a maximum expected magnitude of 7.0–7.2 is obtained. As a reference due to a similar geodynamic setting, though further north with respect to Corfu Island, the Montenegro 1979 earthquake was characterized by a 7.1 magnitude (Boore et al., 1981; Benetatos and Kiratzi, 2006).

The Palaeochori Fault lies instead in the central-eastern portion of transect B, where the tectonic regime is purely extensional and the slip-rate on the normal fault is estimated to be about 0.3 mm/a (Doutsos and Koukouvelas, 1998). An M_w = 6.7–6.8 earthquake struck the area around Kozani-Grevena in 1995, for which the Palaeochori Fault is considered as the causative fault (Resor et al., 2005). Aftershocks are distributed down to depths of ca. 15–16 km (Rigo et al., 2004; Resor et al., 2005), which are consistent with the BDT depth obtained in our rheological modelling (ca. 19–20 km; Figure 12a). Following the procedure described above, the estimated maximum possible magnitude is 6.8–6.9, which is perfectly compatible with the 1995 earthquake. The small discrepancy is likely due to the fact that this event did not produce clear surface ruptures and the associated

Table 2. List of parameters derived from the rheological modelling (BDT depth) and the inferred M_{max} based on the geometrical information from GreDaSS (Caputo and Pavlides, 2013) and applying different empirical relationships (Wells and Coppersmith, 1994). See text for discussion.

	BDT depth [km]	Dip	Width [km]	Length [km]	M_{max}_W	M_{max}_L	M_{max}_RA
Central Offshore Corfu Thrust	20	40–45°	28	56	7.2	7	7.2
Palaeochori Fault	19	65°	21	42	6.8	6.8	6.9
Kalamata Fault	16	60°	18	37	6.7	6.8	6.8
Fili Fault	11	60°	12	25	6.3	6.4	6.5

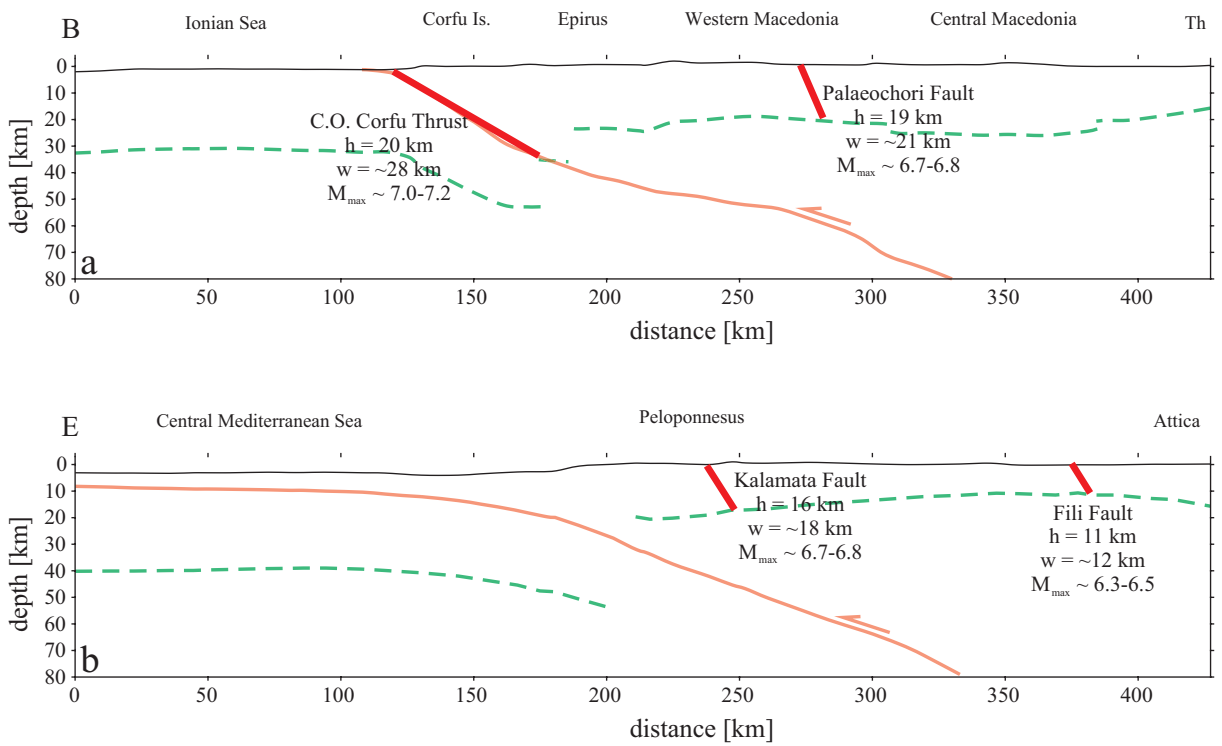

Figure 12. Sketch of some selected seismogenic sources (from GreDaSS; Caputo et al., 2012) crossed by transects B (a) and E (b). For each source the possible maximum dimensions constrained by the BDT depth obtained with the rheological modelling and the corresponding maximum expected magnitude are indicated. COCT = Central Offshore Corfu Thrust; PF = Palaeochori Fault (Kozani-Grevena region); KF = Kalamata Fault; FF = Fili fault.

aftershocks did not occur any shallower than 4 km (Resor et al., 2005), thus suggesting that the coseismic rupture did not propagate across the entire seismogenic layer thickness (in contrast with the assumption of our estimates).

As regards the Kalamata Fault, this lies on the central sector of transect E, where the M_w = 5.8 Kalamata earthquake occurred. The tectonic regime of the region is characterized by WSW-ENE directed extension, almost perpendicular to the strike of the source and the maximum depth extent of the recorded seismicity reaches down to 12–15 km (Lyon-Caen, 1988; Kassaras et al., 2014). Also in this case the seismological data are in agreement with the BDT depth obtained from the rheological modelling, which is about 16 km (Figure 12b). Accordingly, the estimated maximum expected magnitude indicates values around 6.7–6.8, which is consistent with that suggested in GreDaSS (~6.7; Caputo and Pavlides, 2013).

Finally, the Fili Fault is located close to the eastern termination of transect E, in the Attica region near Athens. This tectonic structure is a NW-SE trending normal fault,

dipping SW with an average angle of 55° to 60° (Caputo et al., 2012), and it is considered as the source for the 1999 M_w = 6.0 Athens earthquake (Papadimitriou et al., 2002; Papadopoulos et al., 2002; Ganas et al., 2004). The BDT in this region is quite shallow, with an average depth of 11–12 km (Figure 12b), consistent with the focal depth, determined at 8 km, and the aftershocks not recorded below 11 km (Voulgaris et al., 2001). The maximum expected magnitude obtained on the basis of the rheological BDT is 6.3–6.5, which is slightly greater than the value of the 1999 mainshock. Also in this case, however, it must be taken into account that the rupture only propagated upwards to depths as shallow as 3 km, and therefore the maximum potential magnitude associated with the Fili Fault could be greater in the case of rupture propagation across the entire seismogenic layer.

8. Concluding remarks

Based on a systematic analysis of the available literature data (relative to the principal parameters playing a role in rheological modelling) and exploiting some well-known equations (Equations (1)–(3)), which allow to determine the prevailing bulk behaviour (brittle versus ductile) of rocks, it was possible to reconstruct numerous, closely spaced (ca. 10 km), 1D vertical rheological profiles aligned along several transects across the Hellenides, the Hellenic Arc, and the Aegean region. Numerical modelling has been performed by means of purposely generated MATLAB codes, enabling to calculate at 100-m steps the temperature and strength of rocks in a stratified lithosphere. The vertical information independently obtained for each site was then laterally interpolated along the transects for reconstructing 430- to 450-km-long pseudo-2D sections (Figures 5–8).

In order to compare the different tectonic regimes and geodynamic settings affecting the investigated area, we performed two sets of parallel transects crossing the collisional belt (Albania-Northern Greece) and the subduction zone (Southern Ionian Sea-Peloponnesus), respectively north and south of the Cephalonia Transform Fault (Figure 1). For better constraining the interpretation of the results and thus facilitating the overall analysis, we also reconstructed two longitudinal transects mutually crossing the perpendicular ones.

The results of the numerical modelling allow to determine, for each vertical log and hence laterally along the transects, the depth at which the brittle-ductile transition occurs (graphs (a) in Figures 5–8). For the aims of this paper and as discussed in a previous section, in the event that more than one rheological transition occurred, we selected the shallowest one when at least a 500-m-thick ductile layer separates the two brittle layers. Accordingly, the shallow BDT allows to define the seismogenic layer thickness, which is crucial for seismotectonic analyses.

Overall, the results presented in this paper support the following major conclusions. Firstly, the seismogenic layer thickness, reconstructed along several transects traced across the Aegean region and affecting different tectonic regimes, shows significant lateral variations. Indeed, the depth of the mechanical boundary (including topography/bathymetry) is basically shallower than ca. 20 km in the Aegean microplate, and locally as shallow as 10–12 km in some inner sectors, like central-western Macedonia and the South Aegean Sea (transects D, E, F, and H; Figures 6a and 7a). In contrast, it is systematically deeper in the Nubian plate, where it ranges at 30–35 km in depth in the Apulian block (transects A, B, and C; Figure 5a), and steadily at ca. 40 km within the oceanic lithosphere (transects D, E, and F; Figure 6a). It should be also mentioned that where the subducting plate starts bending and dipping E-NE-wards, the BDT progressively deepens for several tens of kilometres (Figure 10).

In terms of seismotectonic behaviour, it should be also considered that the apparently thick seismogenic layer characterizing the lower plate is likely vertically partitioned by the occurrence of the basal detachment of the continental and oceanic accretionary wedges (Figures 5a and 6a), continuing down-dip into the Wadati–Benioff plane (Figure 3). This major tectonic shear zone, especially in its upper part, certainly consists of very weak sediments and rocks with a high pore fluid pressure (e.g., Davis et al., 1983; Mouchet and Mitchell, 1989; Fertl et al., 1994; Saffer and Tobin, 2011; Suppe, 2014) that mechanically hinder the stress transmission across it. Accordingly, seismogenic ruptures are likely vertically confined also by this important tectonic feature.

A further major conclusion obtained from the numerical modelling is represented by the recognition and geometrical characterization of lithospheric volumes, and even laterally continuous bodies, occurring well below the shallow seismogenic layer, but still behaving brittlely (Figure 10). In principle, when critical stresses here are exceeded, these rock volumes could also generate seismic events. However, their importance in terms of seismic hazard is relatively limited because the possible hypocentres are deeper (and hence both geometric and intrinsic attenuation of the released seismic waves would be greater) and the associated magnitudes are likely reduced due to the generally limited dimensions of these volumes.

By comparing our results, and particularly the reconstructed brittle layers, with the seismicity distribution provided by catalogues with well-located events (Kassaras et al., 2016; NKUA, 2019) and other papers investigating local seismic sequences (Hatzfeld et al., 1995; Resor et al., 2005; Ganas et al., 2012; Mesimeri et al., 2018), the validity of the rheological modelling as a tool for defining

and constraining seismogenic volumes is fully confirmed (Figures 9 and 11). In particular, the choice to consider the shallow BDT as a proxy for crustal seismogenesis seems basically correct. Indeed, the few exceptions of earthquakes occurring outside the seismogenic layer are represented only by small magnitude events reasonably explained in terms of local and/or temporal increases of the pore fluid pressure in particular geodynamic settings. On one hand, these small-scale space variations could be not considered due to the coarser resolution of our model, while the time changes are a priori excluded because of the time-independent approach we used.

Finally, the most important conclusion of this research is probably represented by the crucial inference obtained in terms of seismic hazard assessment and particularly relative to the maximum possible earthquake that a seismogenic source could release. We carried out this exercise for selected major active faults crossing the investigated transects (Figure 1) and affecting different tectonic regimes and geodynamic settings (Figure 12). The obtained inferences based on the rheological modelling are in all cases consistent with independent seismotectonic reviews, as reported in GreDaSS (Caputo et al., 2012; Caputo and Pavlides, 2013), and seismological data associated with recent earthquakes (1986 Kalamata, 1995 Kozani-Grevena, and 1999 Athens events). The slight, though systematic, larger values inferred by our model could be due to the more conservative approach based on the assumption that the entire fault surface could rupture at once (from BDT to Earth's surface). Obviously, magnitudes recorded for recent events could be smaller due to the partial coseismic rupture, either upwards (no linear morphogenic events; Caputo, 2005) or downwards.

As a final statement, we conclude that if particular care is devoted to the collection of the relevant parameters, rheological modelling could represent a powerful tool for characterizing wide regions in terms of seismotectonic behaviour, thus contributing to perform better seismic hazard assessment analyses.

Acknowledgements
We would like to thank the three anonymous reviewers and Editor-in-Chief Orhan Tatar for their constructive comments and suggestions. Research funds to M.M. were from Italian Ministry of University and University of Ferrara (resp. R.C).

References

Armijo R, Lyon-Caen H, Papanastassiou D (1992). East-west extension and Holocene normal-faults scarps in the Hellenic arc. Geology 20: 491-494. doi: 10.1130/0091-7613(1992)020<0491:EWEAHN>2.3.CO;2

Armijo R, Meyer B, King GCP, Rigo A, Papanastassiou D (1996). Quaternary evolution of the Corinth Rift and its implications for the Late Cenozoic evolution of the Aegean. Geophysical Journal International 126: 11-53. doi: 10.1111/j.1365-246X.1996.tb05264.x

Avallone A, Briole P, Agatza-Balodimou AM, Billiris H, Charade O et al. (2004). Analysis of eleven years of deformation measured by GPS in the Corinth Rift Laboratory area. Comptes Rendus Geoscience 336 (4-5): 301-311. doi: 10.1016/j.crte.2003.12.007

Beardsmore GR, Cull JP (editors) (2001). Crustal Heat Flow: A Guide to Measurement and Modelling. 1st ed. Cambridge, UK: Cambridge University Press.

Beeler NM, Hirth G, Tullis TE, Webb CH (2018). On the depth extent of coseismic rupture. Bulletin of the Seismological Society of America 108 (2): 761-780. doi: 10.1785/0120160295

Benetatos C, Kiratzi A (2006). Finite-fault slip models for the 15 April 1979 (M_w 7.1) Montenegro earthquake and its strongest aftershock of 24 May 1979 (M_w 6.2). Tectonophysics 421 (1): 129-143. doi: 10.1016/j.tecto.2006.04.009

Boore DM, Sims JD, Kanamori H, Harding S (1981). The Montenegro, Yugoslavia, earthquake of April 15, 1979: source orientation and strength. Physics of the Earth and Planetary Interiors 27 (2): 133-142. doi: 10.1016/0031-9201(81)90041-8

Brace WF, Kohlstedt DL (1980). Limits on lithospheric stress imposed by laboratory experiments. Journal of Geophysical Research 85 (B11): 6248-6252. doi:10.1029/JB085iB11p06248

Briole P, Rigo A, Lyon-Caen H, Ruegg JC, Papazissi K et al. (2000). Active deformation of the Corinth rift, Greece: results from repeated Global Positioning System surveys between 1990 and 1995. Journal of Geophysical Research 105 (B11): 25605-25625. doi: 10.1029/2000JB900148

Byerlee JD (1968). Brittle-ductile transition in rocks. Journal of Geophysical Research 73 (14): 4741-4750. doi: 10.1029/JB073i014p04741

Byerlee JD (1978). Friction of rocks. In: Byerlee JD, Wyss M (editors). Rock Friction and Earthquake Prediction. 1st ed. Basel, Switzerland: Birkhäuser, pp. 615-626.

Caputo R (2005). Ground effects of large morphogenic earthquakes. Journal of Geodynamics 40 (2-3): 113-118. doi: 10.1016/j.jog.2005.07.001

Caputo R, Chatzipetros A, Pavlides S, Sboras S (2012). The Greek Database of Seismogenic Sources (GreDaSS): state-of-the-art for northern Greece. Annals of Geophysics 55 (5): 859-894. doi: 10.4401/ag-5168

Caputo R, Pavlides S (1993). Late Cainozoic geodynamic evolution of Thessaly and surroundings (central-northern Greece). Tectonophysics 223 (3-4): 339-362. doi: 10.1016/0040-1951(93)90144-9

Caputo R, Pavlides S (2013). The Greek Database of Seismogenic Sources (GreDaSS), Version 2.0.0: A Compilation of Potential Seismogenic Sources (Mw > 5.5) in the Aegean Region. Available at http://gredass.unife.it/. doi: 10.15160/unife/gredass/0200.

Carter NL, Tsenn MC (1987). Flow properties of continental lithosphere. Tectonophysics 136 (1-2): 27-63. doi: 10.1016/0040-1951(87)90333-7

Čermák V (1982). Crustal temperature and mantle heat flow in Europe. Tectonophysics 83 (1-2): 123-142. doi: 10.1016/0040-1951(82)90012-9

Čermak V, Rybach L (1982). Thermal properties: thermal conductivity and specific heat of minerals and rocks. In: Angenheister G (editor). Physical Properties of Rocks. 1st ed. Heidelberg, Germany: Springer, pp. 305-343.

Chapman DS (1986). Thermal gradients in the continental crust. Geological Society of London Special Publications 24 (1): 63-70. doi: 10.1144/GSL.SP.1986.024.01.07

Chen WP, Yu CQ, Tseng TL, Yang Z, Wang CY et al. (2013). Moho, seismogenesis, and rheology of the lithosphere. Tectonophysics 609: 491-503. doi: 10.1016/j.tecto.2012.12.019

Chiaraluce L, Chiarabba C, Collettini C, Piccinini D, Cocco M (2007). Architecture and mechanics of an active low-angle normal fault: Alto Tiberina fault, northern Apennines, Italy. Journal of Geophysical Research 112: B10310. doi: 10.1029/2007JB005015

Chopra PN, Paterson MS (1981). The experimental deformation of dunite. Tectonophysics 78: 453-473. doi: 10.1016/0040-1951(81)90024-X

Cloetingh SAPL, Van Wees JD, Ziegler PA, Lenkey L, Beekman F et al. (2010). Lithosphere tectonics and thermo-mechanical properties: an integrated modelling approach for Enhanced Geothermal Systems exploration in Europe. Earth Science Reviews 102 (3-4): 159-206. doi: 10.1016/j.earscirev.2010.05.003

Collettini C, Holdsworth RE (2004). Fault zone weakening and character of slip along low-angle normal faults: insights from the Zuccale fault, Elba, Italy. Journal of the Geological Society 161 (6): 1039-1051. doi: 10.1144/0016-764903-179

Davis D, Suppe J, Dahlen FA (1983). Mechanics of fold-and-thrust belts and accretionary wedges. Journal of Geophysical Research 88 (B2): 1153-1172. doi: 10.1029/JB088iB02p01153

Dercourt J, Zonenshain LP, Ricou LE, Kazmin VG, Le Pichon X et al. (1986). Geological evolution of the Tethys belt from the Atlantic to the Pamirs since the Lias. Tectonophysics 123: 241-315. doi: 10.1016/0040-1951(86)90199-X

Devoti R, Pietrantonio G, Riguzzi F (2014). GNSS networks for geodynamics in Italy. Física de la Tierra 26: 11-24.

Doglioni C, Carminati E, Petricca P, Riguzzi F (2015). Normal fault earthquakes or graviquakes. Scientific Reports 5: 12110. doi: 10.1038/srep12110

Doser DI, Kanamori H (1986). Depth of seismicity in the Imperial Valley region (1977–1983) and its relationship to heat flow, crustal structure and the October 15, 1979, earthquake. Journal of Geophysical Research 91 (B1): 675-688. doi: 10.1029/JB091iB01p00675

Doutsos T, Koukouvelas I (1998). Fractal analysis of normal faults in northwestern Aegean area, Greece. Journal of Geodynamics 26 (2-4): 197-216. doi: 10.1016/S0264-3707(97)00052-5

Doutsos T, Koukouvelas IK, Xypolias P (2006). A new orogenic model for the External Hellenides. Geological Society of London Special Publications 260 (1): 507-520. doi: 10.1144/GSL.SP.2006.260.01.21

Faccenna C, Becker TW, Auer L, Billi A, Boschi L et al. (2014). Mantle dynamics in the Mediterranean. Reviews of Geophysics 52: 283-332. doi: 10.1002/2013RG000444

Fertl WH, Chapman RE, Hotz RF (editors) (1994). Studies in Abnormal Pressures. Developments in Petroleum Science. 1st ed. Amsterdam, the Netherlands: Elsevier.

Floyd MA, Billiris H, Paradissis D, Veis G, Avallone A et al. (2010). A new velocity field for Greece: implications for the kinematics and dynamics of the Aegean. Journal of Geophysical Research 115: B10. doi: 10.1029/2009JB007040

Fytikas MD, Kolios NP (1979). Preliminary heat flow map of Greece. In: Čermak V, Rybach L (editors). Terrestrial Heat Flow in Europe. Heidelberg, Germany: Springer, pp. 197-205.

Ganas A, Lekkas E, Kolligri M, Moshou A, Makropoulos K (2012). The 2011 Oichalia (SW Peloponnese, Greece) seismic swarm: geological and seismological evidence for EW extension and reactivation of the NNW-SSE striking Siamo fault. Bulletin of the Geological Society of Greece 46: 81-94. doi: 10.12681/bgsg.10927

Ganas A, Pavlides SB, Sboras S, Valkaniotis S, Papaioannou S et al. (2004). Active fault geometry and kinematics in Parnitha Mountain, Attica, Greece. Journal of Structural Geology 26: 2103-2118. doi: 10.1016/j.jsg.2004.02.015

Grigoriadis VN, Tziavos IN, Tsokas GN, Stampolidis A (2016). Gravity data inversion for Moho depth modeling in the Hellenic area. Pure and Applied Geophysics 173 (4): 1223-1241. doi: 10.1007/s00024-015-1174-y

Hansen FD, Carter NL (1982). Creep of selected crustal rocks at 1000 MPa. Transactions of the American Geophysical Union 63: 437.

Hatzfeld D, Kassaras I, Panagiotopoulos D, Amorese D, Makropoulos K et al. (1995). Microseimicity and strain pattern in northwestern Greece. Tectonics 14 (4): 773-785. doi: 10.1029/95TC00839

Hollenstein C, Müller MD, Geiger A, Kahle HG (2008). Crustal motion and deformation in Greece from a decade of GPS measurements, 1993–2003. Tectonophysics 449 (1-4): 17-40. doi: 10.1016/j.tecto.2007.12.006

Hurter S, Haenel R (editors) (2002). Atlas of Geothermal Resources in Europe. Luxembourg City, Luxembourg: Office for Official Publications of the European Communities.

Jackson J, McKenzie D, Priestley K, Emmerson B (2008). New views on the structure and rheology of the lithosphere. Journal of the Geological Society 165 (2): 453-465. doi: 10.1144/0016-76492007-109

Jacobshagen V (editor) (1986). Geologie von Griechenland. 1st ed. Berlin, Germany: Gebrüder Borntraeger (in German).

Kassaras I, Kapetanidis V, Karakonstantis A (2016). On the spatial distribution of seismicity and the 3D tectonic stress field in western Greece. Physics and Chemistry of the Earth, Parts A/B/C 95: 50-72. doi: 10.1016/j.pce.2016.03.012

Kassaras I, Kapetanidis V, Karakonstantis A, Kouskouna V, Ganas A et al. (2014). Constraints on the dynamics and spatio-temporal evolution of the 2011 Oichalia seismic swarm (SW Peloponnesus, Greece). Tectonophysics 614: 100-127. doi: 10.1016/j.tecto.2013.12.012

Kirby SH (1985). Rock mechanics observations pertinent to the rheology of the continental lithosphere and the localization of strain along shear zones. Tectonophysics 119 (1-4): 1-27. doi: 10.1016/0040-1951(85)90030-7

Kind R, Eken T, Tilmann F, Sodoudi F, Taymaz T et al. (2015). Thickness of the lithosphere beneath Turkey and surroundings from S-receiver functions. Solid Earth 6: 971-984. doi: 10.5194/se-6-971-2015

Kirby SH, Kronenberg AK (1987). Rheology of the lithosphere: selected topics. Reviews of Geophysics 25 (6): 1219-1244. doi: 10.1029/RG025i006p01219

Kopf A, Mascle J, Klaeschen D (2003). The Mediterranean Ridge: A mass balance across the fastest growing accretionary complex on Earth. Journal of Geophysical Research 108 (B8): 2372. doi: 10.1029/2001JB000473

Koukouvelas IK, Aydin A (2002). Fault structure and related basins of the North Aegean Sea and its surroundings. Tectonics 21: 1046. doi: 10.1029/2001TC901037

Kreemer C, Blewitt G, Klein EC (2014). A geodetic plate motion and Global Strain Rate Model. Geochemistry, Geophysics, Geosystems 15 (10): 3849-3889. doi: 10.1002/2014GC005407

Le Pichon X, Angelier J (1979). The Hellenic arc and trench system: a key to the neotectonic evolution of the eastern Mediterranean area. Tectonophysics 60 (1-2): 1-42. doi: 10.1016/0040-1951(79)90131-8

Lyon-Caen H, Armijo R, Drakopoulos J, Baskoutass J, Delibassis N et al. (1988). The 1986 Kalamata (South Peloponnesus) earthquake: detailed study of a normal fault, evidences for east-west extension in the Hellenic arc. Journal of Geophysical Research 93: 14967-15000. doi: 10.1029/JB093iB12p14967

Makris J, Papoulia J, Yegorova T (2013). A 3-D density model of Greece constrained by gravity and seismic data. Geophysical Journal International 194 (1): 1-17. doi: 10.1093/gji/ggt059

Makropoulos K, Kaviris G, Kouskouna V (2012). An updated and extended earthquake catalogue for Greece and adjacent areas since 1900. Natural Hazards and Earth System Sciences 12 (5): 1425-1430. doi: 10.5194/nhess-12-1425-2012

McKenzie D (1972). Active tectonics of the Mediterranean Region. Geophysical Journal of the Royal Astronomical Society 30: 109-185. doi: 10.1111/j.1365-246X.1972.tb02351.x

McKenzie D, Jackson J, Priestley K (2005). Thermal structure of oceanic and continental lithosphere. Earth and Planetary Science Letters 233 (3-4): 337-349. doi: 10.1016/j.epsl.2005.02.005

Mercier JL (1976). La neotectonique. Ses methodes et ses buts. Un exemple: l'Arc Egéen (Méditerranée orientale). Revue de Géographie Physique et de Géologie Dynamique 18 (4): 323-346 (in French).

Mercier JL, Sorel D, Vergely P, Simeakis K (1989). Extensional tectonic regimes in the Aegean basins during the Cenozoic. Basin Research 2 (1): 49-71. doi: 10.1111/j.1365-2117.1989.tb00026.x

Mesimeri M, Karakostas V (2018). Repeating earthquakes in western Corinth Gulf (Greece): implications for aseismic slip near locked faults. Geophysical Journal International 215 (1): 659-676. doi: 10.1093/gji/ggy301

Middleton TA, Copley A (2014). Constraining fault friction by re-examining earthquake nodal plane dips. Geophysical Journal International 196 (2): 671-680. doi: 10.1093/gji/ggt427

Mouchet JP, Mitchell A (editors) (1989). Abnormal Pressures While Drilling. 1st ed. Boussens, France: Elf Aquitaine.

Mountrakis D (2006). Tertiary and Quaternary tectonics of Greece. In: Dilek Y, Pavlides S (editors). Postcollisional tectonics and magmatism in the Mediterranean region and Asia. Geological Society of America Special Papers 409: 125-136.

Muço B (1994). Focal mechanism solutions for Albanian earthquakes for the years 1964-1988. Tectonophysics 231 (4): 311-323. doi: 10.1016/0040-1951(94)90041-8

Müller MD, Geiger A, Kahle HG, Veis G, Billiris H et al. (2013). Velocity and deformation fields in the North Aegean domain, Greece, and implications for fault kinematics, derived from GPS data 1993–2009. Tectonophysics 597: 34-49. doi: 10.1016/j.tecto.2012.08.003

Nocquet JM (2012). Present-day kinematics of the Mediterranean: A comprehensive overview of GPS results. Tectonophysics 579: 220-242. doi: 10.1016/j.tecto.2012.03.037

NOA (2017). Full Catalogue 1964-2017. Athens, Greece: National Observatory of Athens. Available at www.gein.noa.gr/en/seismicity/earthquake-catalogs.

Olhoeft GR, Johnson GR (1989). Densities of rocks and minerals. In: Carmichael RS (editor). Practical Handbook of Physical Properties of Rocks and Minerals. 1st ed. Boca Raton, FL, USA: CRC Press, pp. 1-38.

Papadimitriou P, Voulgaris N, Kassaras I, Kaviris G, Delibassis N et al. (2002). The M_w=6.0, 7 September 1999 Athens earthquake. Natural Hazards 27 (1): 15-33. doi: 10.1023/A:1019914915693

Papadopoulos GA, Ganas A, Pavlides S (2002). The problem of seismic potential assessment: Case study of the unexpected earthquake of 7 September 1999 in Athens, Greece. Earth, Planets and Space 54: 9-18. doi: 10.1186/BF03352417

Papanikolaou D (2013). Tectonostratigraphic models of the Alpine terranes and subduction history of the Hellenides. Tectonophysics 595: 1-24. doi: 10.1016/j.tecto.2012.08.008

Papazachos C (1999). An alternative method for a reliable estimation of seismicity with an application in Greece and the surrounding area. Bulletin of the Seismological Society of America 89 (1): 111-119.

Pérouse E, Chamot-Rooke N, Rabaute A, Briole P, Jouanne F et al. (2012). Bridging onshore and offshore present-day kinematics of central and eastern Mediterranean: implications for crustal dynamics and mantle flow. Geochemistry, Geophysics, Geosystems 13: Q09013. doi: 10.1029/2012GC004289

Petricca P, Barba S, Carminati E, Doglioni C, Riguzzi F (2015). Graviquakes in Italy. Tectonophysics 656: 202-214. doi: 10.1016/j.tecto.2015.07.001

Ranalli G (editor) (1995). Rheology of the Earth. 2nd ed. London, UK: Chapman and Hall.

Ranalli G, Murphy DC (1987). Rheological stratification of the lithosphere. Tectonophysics 132 (4): 281-295. doi: 10.1016/0040-1951(87)90348-9

Reicherter K, Hoffmann N, Lindhorst K, Krastel S, Fernández-Steeger T et al. (2011). Active basins and neotectonics: morphotectonics of the Lake Ohrid Basin (FYROM and Albania). Zeitschrift der Deutschen Gesellschaft für Geowissenschaften 162 (2): 217-234. doi: 10.1127/1860-1804/2011/0162-0217

Resor PG, Pollard DD, Wright TJ, Beroza GC (2005). Integrating high-precision aftershock locations and geodetic observations to model coseismic deformation associated with the 1995 Kozani-Grevena earthquake, Greece. Journal of Geophysical Research 110: B09402. doi: 10.1029/2004JB003263

Rigo A, de Chabalier JB, Meyer B, Armijo R (2004). The 1995 Kozani-Grevena (northern Greece) earthquake revisited: an improved faulting model from synthetic aperture radar interferometry. Geophysical Journal International 157: 727-736. doi: 10.1111/j.1365-246X.2004.02220.x

Ring U, Glodny J, Will T, Thomson S (2010). The Hellenic subduction system: high-pressure metamorphism, exhumation, normal faulting, and large-scale extension. Annual Review of Earth and Planetary Sciences 38: 45-76. doi: 10.1146/annurev.earth.050708.170910

Robertson AHF, Clift PD, Degnan PJ, Jones G (1991). Palaeogeographic and palaeotectonic evolution of the Eastern Mediterranean Neotethys. Palaeogeography, Palaeoclimatology, Palaeoecology 87: 289-343. doi: 10.1016/0031-0182(91)90140-M

Rolandone F, Bürgmann R, Nadeau RM (2004). The evolution of the seismic-aseismic transition during the earthquake cycle: constraints from the time-dependent depth distribution of aftershocks. Geophysical Research Letters 31: L23610. doi: 10.1029/2004GL021379

Royden LH, Papanikolaou DJ (2011). Slab segmentation and late Cenozoic disruption of the Hellenic arc. Geochemistry, Geophysics, Geosystems 12: Q03010. doi: 10.1029/2010GC003280

Rutter EH (1986). On the nomenclature of mode of failure transitions in rocks. Tectonophysics 122 (3-4): 381-387. doi: 10.1016/0040-1951(86)90153-8

Sachpazi M, Laigle M, Charalampakis M, Diaz J, Kissling E et al. (2016). Segmented Hellenic slab rollback driving Aegean deformation and seismicity. Geophysical Research Letters 43: 651-658. doi: 10.1002/2015GL066818

Saffer DM, Tobin HJ (2011) Hydrogeology and mechanics of subduction zone forearcs: fluid flow and pore pressure. Annual Review of Earth and Planetary Sciences 39: 157-186. doi: 10.1146/annurev-earth-040610-133408

Scholz CH (1988). The brittle-plastic transition and the depth of seismic faulting. Geologische Rundschau 77 (1): 319-328. doi: 10.1007/BF01848693

Şengör AMC (1985). The story of Tethys: How many wives did Okeanos have? Episodes 8: 3-12.

Shelton G, Tullis JA (1981). Experimental flow laws for crustal rocks. Transactions of the American Geophysical Union 62: 396.

Sibson RH (1974). Frictional constraints on thrust, wrench and normal faults. Nature 249 (5457): 542. doi: 10.1038/249542a0

Sibson RH (1977). Fault rocks and fault mechanisms. Journal of the Geological Society 133 (3): 191-213. doi: 10.1144/gsjgs.133.3.0191

Sibson RH (1982). Fault zone models, heat flow, and the depth distribution of earthquakes in the continental crust of the United States. Bulletin of the Seismological Society of America 72 (1): 151-163.

Sodoudi F, Kind R, Hatzfeld D, Priestley K, Hanka W et al. (2006). Lithospheric structure of the Aegean obtained from P and S receiver functions. Journal of Geophysical Research 111: B12307. doi: 10.1029/2005JB003932

Suppe J (2014). Fluid overpressures and strength of the sedimentary upper crust. Journal of Structural Geology 69: 481-492. doi: 10.1016/j.jsg.2014.07.009

Taymaz T, Jackson J, McKenzie DP (1991). Active tectonics of the north and central Aegean Sea. Geophysical Journal International 106: 433-490. doi: 10.1111/j.1365-246X.1991.tb03906.x

Taymaz T, Westaway R, Reilinger R (2004). Active faulting and crustal deformation in the Eastern Mediterranean region. Tectonophysics 391 (1): 1-10. doi: 10.1016/S0040-1951(04)00402-0

Tesauro M, Kaban MK, Cloetingh SA (2008). EuCRUST-07: A new reference model for the European crust. Geophysical Research Letters 35: L05313. doi: 10.1029/2007GL032244

Tesauro M (2009). An integrated study of the structure and thermomechanical properties of the European lithosphere. PhD, Vrije Universiteit, Amsterdam, the Netherlands.

Tiberi C, Diament M, Lyon Caen H, King T (2001). Moho topography beneath the Corinth Rift area (Greece) from inversion of gravity data. Geophysical Journal International 145 (3): 797-808. doi: 10.1046/j.1365-246x.2001.01441.x

Tirel C, Gueydan F, Tiberi C, Brun JP (2004). Aegean crustal thickness inferred from gravity inversion. Geodynamical implications. Earth and Planetary Science Letters 228 (3-4): 267-280. doi: 10.1016/j.epsl.2004.10.023

Turcotte D, Schubert G (editors) (2014). Geodynamics. 3rd ed. Cambridge, UK: Cambridge University Press.

van Hinsbergen DJJ, Hafkenscheid E, Spakman W, Meulenkamp JE, Wortel R (2005). Nappe stacking resulting from subduction of oceanic and continental lithosphere below Greece. Geology 33 (4): 325-328. doi: 10.1130/G20878.1

Vernant P, Reilinger R, McClusky S (2014). Geodetic evidence for low coupling on the Hellenic subduction plate interface. Earth and Planetary Science Letters 385: 122-129. doi: 10.1016/j.epsl.2013.10.018

Vilà M, Fernández M, Jiménez-Munt I (2010). Radiogenic heat production variability of some common lithological groups and its significance to lithospheric thermal modeling. Tectonophysics 490 (3-4): 152-164. doi: 10.1016/j.tecto.2010.05.003

Voulgaris N, Pirli M, Papadimitriou P, Kassaras J, Makropoulos K (2001). Seismotectonic characteristics of the area of western Attica derived from the study of the September 7, 1999 Athens earthquake aftershock sequence. Bulletin of the Geological Society of Greece 34 (4): 1645-1651. doi: 10.12681/bgsg.17274

Wells DL, Coppersmith JK (1994). New empirical relationships among magnitude, rupture length, rupture width, rupture area, and surface displacement. Bulletin of the Seismological Society of America 84: 974-1002.

Wessel P, Smith WH (1991). Free software helps map and display data. Eos, Transactions American Geophysical Union 72 (41): 441-446.

Yolsal-Çevikbilen S, Taymaz T (2012). Earthquake source parameters along the Hellenic subduction zone and numerical simulations of historical tsunamis in the Eastern Mediterranean. Tectonophysics 536: 61-100. doi: 10.1016/j.tecto.2012.02.019

Zelt BC, Taylor B, Sachpazi M, Hirn A (2005). Crustal velocity and Moho structure beneath the Gulf of Corinth, Greece. Geophysical Journal International 162 (1): 257-268. doi: 10.1111/j.1365-246X.2005.02640.x